LUND UNIVERSITY

Control of Hybrid Electric Vehicles with Diesel Engines

Jonasson, Karin

2005

Control of Hybrid Electric Vehicles with Diesel Engines

Karin Jonasson

LUND UNIVERSITY

Doctoral Dissertation in Industrial Electrical Engineering

Department of Industrial Electrical Engineering and Automation

Abstract

This thesis is an approach to improve electric hybrid vehicles with respect to fuel consumption and to fulfil the future intended NO_X emission regulations. It is based upon the conclusions made in the licentiate thesis *Analysing Hybrid Drive System Topologies* (Jonasson, 2002).

The study in this thesis is restricted to a parallel hybrid vehicle equipped with a diesel engine, two electric machines and electrical energy storage and a model thereof is presented in the thesis.

The choice to focus on the diesel engine is related to the high efficiency of this engine that also is the reason for the in later years increased market for diesel engines in conventional vehicles. Since one of the disadvantages, related to the diesel engine, are the nitrogen oxides (NO_X) emissions, efforts is concentrated on reducing them, by means of the advantages of hybridisation.

The reference vehicle in the simulations presented in this thesis is a Toyota Prius, an electric hybrid passenger car, which is available on the market today. As input for the combustion engine model, engine data from a diesel engine considered as state of the art 2004, has been used. The engine data is scaled to correspond to the engine size used in the Prius. It should be mentioned that the engine in the Toyota Prius is run on petrol.

There are many possible parameters in the simulation model, which are adjustable; vehicle chassis parameters, engine, electric machine(s) and battery size and types, losses models, charging strategies and driver behaviour etc. A number of key parameters have been selected in this study: control strategy, NO_X control by means of EGR (exhaust gas recirculation) and SCR (selective catalytic reduction), gear ratios and gearshift strategies and finally cylinder deactivation. The accuracy of the

simulation model is ratified by means of measured data on the engine used in the simulation.

Fuel consumption and NO_X are determined by using look-up-tables based on measured data. The engine temperature, needed to determine the NO_X conversion by means of SCR, is also received from a look-up-table.

The simulation model is evaluated in the driving cycle ECE+EUDC.

The results presented are chosen to illustrate the impact each individual parameter has on the behaviour of the hybrid vehicle, the fuel consumption and the emissions.

The results from the simulations show that it is possible to pass the expected limit of the future Euro 5 NO_X regulations, if NO_X emission treatment with EGR and SCR is implemented. The price to pay for this action is to sacrifice some of the fuel savings that the hybridization brings. The result is nevertheless a vehicle with decreased fuel consumption compared with a conventional diesel powered vehicle, and a vehicle that passes the intended emission regulation.

Acknowledgements

The goal of this long journey is finally here. The journey ends. But, to use a known speech:

> *This is not the end. It is not even the beginning of the*
> *end. But it is, perhaps, the end of the beginning.*[1]

The thesis is written and time will show what lies ahead. Anyhow, this thesis had not been completed without support from my fellow workers and dear beloved friends and family, some of which I would like to mention especially.

Somewhere in between board meetings, ailing children, lectures and telephone meetings my supervisor Professor Mats Alaküla, at the Department of Industrial Electrical Engineering and Automation, somehow always finds a minute or two. I would like to thank him for his encouragement, patience and enthusiasm and for never doubting in my capacity.

This thesis covers different fields of research, and without the precious support from Dr Rolf Egnell, at the Department of Heat and Power Engineering, it would not have been possible to carry through. Calling me from Greece, e-mailing me from fishing for crayfish and answering the phone when restoring his veteran cars - there is simply nothing that prevents him from contribute with support, a piece of good advice or necessary knowledge. Enthusiasm cannot be bought for money, but it is contagious. I thank him for all the interest he has shown in my struggle with this thesis.

---

[1] Sir Winston Churchill at the Lord Mayor´s Luncheon, Manison House, London, November 10, 1942.

Contents

Chapter 1

Introduction

This thesis is an approach to improve electric hybrid vehicles with respect to fuel consumption and to fulfil the future intended NO_X emission regulations. It is based upon the conclusions drawn in the licentiate thesis *Analysing Hybrid Drive System Topologies* (Jonasson, 2002). The following can be considered as a continuation of the work presented there, with focus changed towards ICE (internal combustion engine) specific control aspects and diesel engines.

1.1 Problem framing

Electric hybridisation of combustion engine vehicles gives new degrees of freedom that are not available in conventional vehicles. The idea behind this thesis is to take advantage of some options of hybridisation of parallel hybrid vehicles with diesel motors, in particular aspects related to the control of the ICE. The choice to focus on the diesel engine is related to the high efficiency of this engine that also is the reason for the later years increased market for diesel engines in conventional vehicles. Since one of the disadvantages, related to the diesel engine, are the nitrogen oxides (NO_X) emissions, efforts will be concentrated on reducing them. The accuracy of the simulation model will be ratified by means of measured data connected to the motor data used in the simulation.

The engine, from where the measured data origin, is equipped with a system for particulate treatment by particulate filter. Therefore the issue

with particulate is considered as sufficiently worked out and is not further dealt with in this study.

1.2 Driving forces

The oil resources in the world are decreasing. The speed thereof is debated but not the fact that the oil is a limited natural resource. The pollution, which derives from combustion of fossil hydrocarbons, causes health problems and accelerates the greenhouse effect. The oil price on the world market has been quoted for new top levels lately due to war, strikes and other political issues. There are, in other words, several reasons, which affect the whole society, to work for decreasing fuel consumption and the damaging effects thereof.

1.3 Objectives

The objective of this thesis is to find control methods that contribute to reduce the fuel consumption and the NO_X emissions from a diesel electric parallel hybrid vehicle. The results of these efforts will be compared with a conventional vehicle and to measured data.

The simulation models are furthermore made disregarding the long-term effects that can affect the vehicle components. Neither is a cost estimation included in the model.

1.4 Criticism of the sources

When comparing commercial systems, there are always obstacles in the efforts of finding relevant component data, since they are surrounded by secrecy. The used engine data used for this study has to be considered as top of the line. Its source is not to be revealed in return. To fit the prevailing task the engine data have been scaled to the correct size.

Running the ICE in transient or in steady state mode makes a difference for example regarding the charging pressure. The turbo charger might not keep up with the transient changes in fuel flow. This affects mainly the formation of particulates and carbon monoxides, which become underestimated in calculations due to the lack of oxygen. The nitrogen oxides are relatively unaffected by the transients. Since the chosen driving cycle do not include significant transients, a simulation may be expected to

indicate fuel consumption and emissions different from those of reality. However in comparison with equivalent measured data the model does not show significant deviation in fuel consumption and nitrogen oxides, the interests in focus of this study. Thus the ICE model used in this thesis is reasonably accurate for the purpose of estimating fuel consumption and NO_X emissions.

Data for Selective Catalytic Reduction (SCR) is obtained from measurements from other engine tests. These results are implemented in the simulation model.

1.5 Literature overview

Electric machines and internal combustion engines are inventions with more than a century on the open market. This implies that they have undertaken numerous of improvements and have been the subject of other hardly happy experiments. Since this thesis focusing on control of hybrid electric vehicles with diesel engines, the literature mentioned below will only touch on subjects related to this.

Hybrid vehicles

Hybrid vehicles include a number of different solutions. There is a potential of efficiency savings to gain when implementing secondary energy storage (Imai et al., 1997). Except vehicles equipped with combustion engine and electric machines, there are HEVs that consist of an electric machine and pedal power (Twike, 2005) as well as air hybrids using compressed air in combination with fossil fuel (Schechter 1996 and Andersson, 2004b).

There are many possible solutions to choose between when implementing hybridization in a vehicle (Baretta, 1998). In (Hellgren, 2004) an attempt is made to unbiased evaluate different solutions. In (Jonasson, 2002) four hybrid topologies are evaluated and in (Bolognesi et al., 2001) another attempt to evaluate hybrid electric drive trains is presented. A comparison of several powertrain technologies is carried out in (Atkins et al., 2003).

Improvements, concerning fuel economy and emissions, are performed on a passenger hybrid electric car, which is available on the market, is presented in (Muta et al., 2004). The benefits gained when implementing CVT in a hybrid vehicle is studied in (Gomez et al., 2004).

Control algoritms

The control of the primary and secondary energy storages in the hybrid vehicle is crucial for the fuel consumption and the emission formation. There are examples of control algorithms that are intuitive (Jonasson, 2002) and those who are more complex (Hellgren, 2004, and Rutquist et al., 2004). In (Hellgren – Jonasson, 2004) an intuitive algorithm is compared with a more complex algorithm. The differences in results regarding fuel consumption turn out to be small. Other comparisons of control algorithms are discussed in (Van Mierlo et al., 1998, Bengtsson, 2004, Wang – Zhang, 2004, Han et al., 2004 and Van Mierlo – Gaston, 2000).

The possibilities to utilize a known driving pattern when controlling the power distribution, such as a specific bus route, is studied in (Andersson et al., 2000b). Control algorithms developed for military vehicles are discussed in (Liang et al., 2003).

Diesel engines and emission treatment

Implementing diesel engines in hybrid electric vehicles presents new challenges. An attempt to achieve the best fuel economy, engine life and lowest emission with an experimental set-up of a single cylinder diesel engine can be studied in (Al-Atabi – Yusaf, 2002).

Non-linear mathematical models, which map the transient and steady state behaviour of diesel electric drivetrains and their components, are developed and validated with experimental results (Lyshevski, 1999).

The drawbacks with the diesel engine are the emissions. Attempts to treat the NO_X emissions using multiple-injections can be studied in (Han et al., 1996 and Chan et al., 1997). Other studies are aiming at implementing EGR (Green, 2000 and Egnell, 2001) and yet others are using SCR to treat the NO_X emissions (Chandler, 2000, Gieshoff et al., 2000, Künkel, 2001 and Andersson et al., 1994).

1.6 Main results

This thesis contains results from simulation aiming to improve electric hybrid vehicles with respect to fuel consumption and to fulfil the future intended NO_X emission regulations. Actions have been carried out on

control strategies for the choice of load points, emission control (EGR and SCR), gearshift control and cylinder deactivation.

The main conclusion is that if a hybrid vehicle is implemented, it has to be implemented with control algorithms taking not only general energy flow aspects into account, but also the emission and fuel consumption properties of the ICE. If only the control structures aimed at conventional vehicles were to be used for hybrid vehicles, the potential of hybrid systems would not at all be utilized.

1.7 Outline of the thesis

This Chapter contains a problem framing, the objectives, a summary of the main results as well as a brief introduction to the thesis.

In chapter 2, the pros and cons of conventional and hybrid vehicles are described. A number of hybrid topologies are presented as well as primary and secondary energy converters.

Chapter 3 elucidate fuel consumption and emissions associated with combustion of hydrocarbon fuels. The chapter also describes possible treatment methods to reduce the emissions.

Actions making it possible to control the electric hybrid system are described in Chapter 4. In this chapter it is also analysed how an improvement of the system can be measured.

The simulation model used is described in Chapter 5 as well as how the control algorithm is implemented in the model.

The results are given in Chapter 6 as well as a description of the reference vehicle that has been used.

In Chapter 7 the conclusions and the future work are described, followed by references in Chapter 8. The appendices include nomenclature and abbreviations.

Chapter 2

Hybrid systems

A hybrid is something that has two different types of components performing essentially the same function. (Your Dictionary, 2001) In this case it is an electrical machine and a combustion engine that together, or one at a time, provide the tractive power to the vehicle. But why hybrid vehicles when there are conventional vehicles that can cope up with the task just fine?

2.1 Motivations for hybrid systems

In conventional vehicles the combustion engine must choose operating load point that corresponds to the instantaneous demanded tractive power. Since the ICE does not provide power with high efficiency at all operating points, in particularly not at low loads, and most modern vehicles are significantly over powered, the efficiency at average (=low power) driving conditions is relatively low.

Furthermore, conventional vehicles have no possibilities to avoid load points that have a disadvantageous emission formation. Sudden load increasments causes transients when the engine tries to follow them and it includes also transiently raised emissions due to a sudden increase of injected fuel.

When braking, there are small possibilities to recover energy in a conventional vehicle. Almost all kinetic energy, originating from the fuel energy, will be lost.

The electric hybrid vehicles, on the other hand, have the advantage to alter its tractive power sources or even better the possibility to combine them. This leads to the possibility to slow down the changes of load points for the ICE. By utilizing pure electric mode it is possible to avoid low ICE efficiency or load points that forms large amount of emissions, if combining the ICE and electric machine does not solve the problem. Furthermore, the presence of a battery makes it possible to regenerate braking energy.

The pure electric vehicles (EV) are still not ready to conquer the market from the conventional vehicles, even though battery performance of both NiHM and LiO technologies have improved significantly during the later years. The main reason for not building pure electric vehicles is still the shortcoming of the batteries. The energy supply is simply not enough for longer trips. On top of this comes that the time needed for recharging the batteries is not negligible. A 6 hour coffee brake after 50-80 km might not be efficient at long trips. Therefore a hybrid of today combines the extended range of a conventional vehicle with the environmental benefits of an electrical vehicle. This results in a vehicle with improved fuel economy and lowered, yet not zero, emissions (How stuff works, 2001a). The main drawback with a HEV is the price that is higher due to increased complexity.

The goal, to minimize the use of non-efficient operating points, is more or less easy to achieve depending on the chosen hybrid topology.

2.2 Topologies

In hybrid vehicles, studied in this thesis, there are one combustion engine and, at least, one electric machine. The engine can be of petrol or diesel type. The hybrid vehicles also include an energy buffer, in this study a chemical battery. It can though be e.g. a. mechanical battery (flywheel), electrostatic (capacitor) or pneumatic (pressurized air).

There are many ways of combining the included components and consequently the number of possible hybrid topologies is large, considering the combinations of electric machines, gearboxes, clutches etc. (Harbolla, 1992). The two main solutions, series and parallel topology, can be supplemented in a numerous amount of combinations, each one with its pros and cons. The other topologies can, strongly simplified, be described as variants of these two basic concepts. The topology efficiency is

depending on the chosen vehicle solution with its unique characteristics and the actual working condition.

Parallel
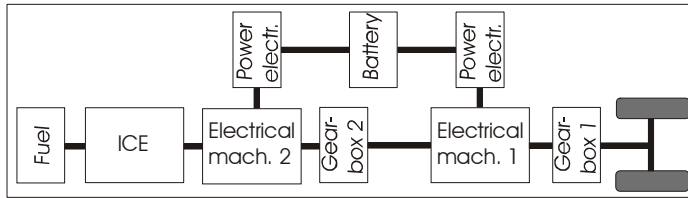
Figure 2.1: Parallel hybrid topology with one optional electric traction motor.

The parallel hybrid is a combination of drive systems (see Figure 2.1) The ICE is mechanically connected to the wheels via a gearbox. The gearbox (no.2) used in the simulations, has 6 steps. Gearbox 1 is given a fixed gear ratio. The low number of power conversions can potentially increase the efficiency of the vehicle as compared to a series hybrid (see below).

The load point, i.e. speed and torque combination of the ICE, of the hybrid can to some extent be chosen freely with the help of the electrical machines, i.e. the speed of the ICE is chosen with the gearbox(es) and the torque with the electric machine(s). There are four options available: pure electric operation, pure ICE operation, electric operation while ICE is charging the battery and finally operation with all power sources. To achieve peak tractive power, both the ICE and the electric machines are used. The parallel topology is also possible to achieve with only one electric machine.

A relative to the parallel topology is the dual mode hybrid where the electric motors drive the vehicle via one axle each (Van Mierlo, 2000 and Nordlund, 2003).

Series
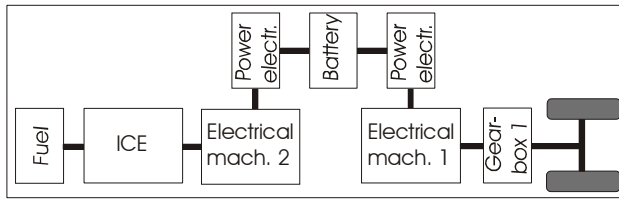
Figure 2.2:   Series hybrid topology.

The series hybrid has no mechanical connection between the ICE and the wheels. The ICE load point can therefore be chosen freely, but at the expense of more energy conversions than with the parallel hybrid. The thermal energy is converted into mechanical energy in the ICE, and thereafter, in the generator, turned into electric energy. The generator charges the battery that in its turn supplies the power electronics for the electric traction motor(s). On its way the energy also passes power electronics twice, in the worst case. These many energy conversions cause the topology a significant reduction of the system efficiency. The ICE efficiency is depending on the low pass filtered power demand.

 The electric machine 1 in Figure 2.2, i.e. the traction motor, has to be designed for peak power and the generator is designed for the ICE power. The simplest series hybrid vehicle is an electric vehicle, equipped with a range extender.

An advantage with the topology is that the ICE can be turned off when the vehicle is driving in a zero-emission zone, but this can be accomplished with a parallel hybrid as well. Yet another merit of the series topology is that the ICE and the electric machine can be mounted separately. This involves a possibility to distribute the weight of the vehicle drive system and in buses an opportunity to use low floor (Hemmingsson, 1999, Van Mierlo et al., 1998 and Nordlund, 2003).

Power split
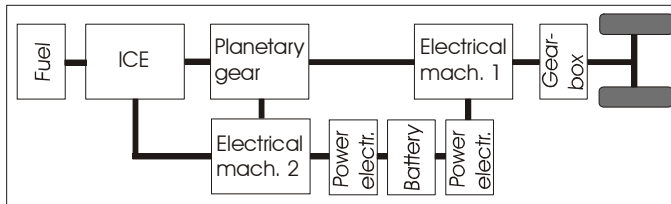
Figure 2.3:   Power split hybrid topology.

The Power Split Hybrid (PSH) has a blurred transformation between the series and parallel hybrid state (Figure 2.3)(Andreasson, 2004). The PSH is even called complex, combined or dual hybrid vehicle.

A planetary gearbox (Figure 2.4) connects the two electrical machines and the ICE. The traction motor (electric machine 1) is connected to the ring wheel, the generator (electric motor 2) to the solar wheel and finally the ICE is connected to the carrier and thereby possible to switch off and the vehicle can operate in a pure electric mode. Owing to the connection of the sun wheel and the planet wheels the speed of the engine can simply be adjusted by varying the speed of the generator.
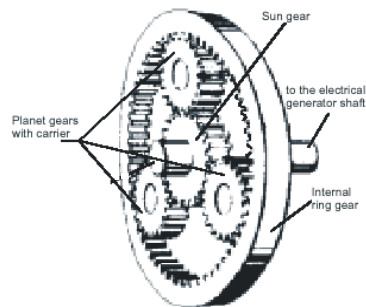
Figure 2.4:   Planetary gear. The numbers of planet wheels are variable but influence the equations.

At most operating points some of the prime energy flows from the ICE to the wheels via the gearbox as in a parallel hybrid, and some flows via the electrical machines as in a series hybrid. The proportion between these two energy flows is speed dependent and at a certain speed it works as a pure parallel hybrid. In most other operating points it's partially a parallel hybrid

and partially a series hybrid. The latter means several conversions of the energy that flows the "series" way from the prime energy source to the wheels. This hints that it is difficult to get the system efficiency higher than the parallel hybrid efficiency.

There are many possible combinations of a PSH. While using reduction gears, CVT, advanced planetary gear, clutches and different numbers of motors the possible number of combinations grows rapidly. The drawback with the topology is that it can cause a power vicious circle that cost unnecessary high transmission losses.

2.3 Primary energy sources

As the name hybrid indicates, there are a combination of tractions systems. In this study the focus has been on diesel electric hybrids. The most common power units will be described below.

Efficiency is a standard of the relation of the capability to transform input to output, such as fuel to kinetic energy. The theoretical efficiency of a spark ignition engine (otto) is given in Equation 2.1. An ordinary otto engine has maximum efficiency of around 33%, while the efficiency of a Diesel engine is approximately 42% (due to higher compression ratio, ε).

$$\eta_t = 1 - \frac{1}{\varepsilon^{\kappa-1}} \tag{2.1}$$

η_t = maximal theoretical efficiency of a piston engine (ICE), ε = compression ratio of an ICE, κ = the ratio of specific heats (= c_p/c_v), c_p = specific heat of a gas at constant pressure, c_v = specific heat of a gas at constant volume

Increasing ε involves increasing friction losses. Therefore the results do not necessarily lead to higher efficiency. The temperature also affects the efficiency. The mechanical efficiency is described in Equation 2.2.

$$\eta_m = 1 - \frac{FMEP}{IMEP_n} \tag{2.2}$$

η_m = mechanical efficiency of an ICE, $FMEP$ = friction mean effective pressure, $IMEP_n$ = indicated mean pressure of a combustion engine (n = net)

As $IMEP_n$ is increased, η_m increases too. This is possible by increasing the load, which implies a higher torque. The ICE efficiency is therefore higher at high torque and not too high rotational speed. The latter is due to that FMEP increases rapidly with increasing speed.

The efficiency of a hybrid vehicle is not only depending on the efficiency of the primary power unit but also on the electric machines, the battery, the transmissions and the power electronics etc. The specific choice of the single components and system control makes up the total efficiency. The total efficiency is inversely proportional to the specific fuel consumption (Heilig, 1985, Johansson, 1999, Bäckström, 2000).

Petrol (Otto) engines

The air/fuel mixture used in modern petrol engines is stochiometric, i.e. $\lambda = 1.0$. The reason for this is the function of the three-way catalyst (TWC).

The throttle, an air valve in the intake manifold that varies the flow of fuel to the combustion chambers of the cylinders, regulates the amount of the air/fuel mixture.

An ignition system is used to ignite the mixture by means of using a spark plug mounted in one of the openings to the combustion chamber.

A developed version of this engine, injects the fuel directly into the cylinders. This is referred to as GDI, Gasoline[2] Direct Injection, and thus the inlet ports only convey air, and EGR if any, into the combustion chamber. (Johansson, 1999 and Alaküla, 2004)

Diesel engines

The other main type of reciprocating piston engine is the diesel engine. Diesel fuel is a petroleum oil fraction heavier than petrol. The diesel engine uses the heat produced by compression rather than a spark, from a sparkplug, to ignite the injected diesel fuel. The fuel is injected directly into the combustion chamber in the modern diesel engine, like in the GDI engine mentioned above. The lack of an electrical ignition system improves the reliability of the engine.

---

[2] petrol (br. eng) or gasoline (am. eng.)

Diesel engines have no throttle and thus the power output is regulated with the quantity of fuel only. There is more air than needed for complete combustion present in the combustion chamber. The extra strength required containing the higher temperatures and pressures and lower speeds causes diesel engines to be heavier than petrol engines with the same power.

The increased fuel economy of the diesel compared to the petrol engine means that the diesel produces less carbon dioxide (CO_2) measured per covered distance. Unburnt carbon in diesel engine produce black soot in the exhaust. Other problems associated with the exhaust gases (high particulates including soot and nitrogen oxide) can be lowered with improved engine control.

The addition of a turbocharger or supercharger to the engine greatly assists in increasing fuel economy and power output. Diesel engines are most widely used where large amounts of power are required: heavy trucks, locomotives, and ships (Johansson, 1999 and Alaküla, 2004).

The otto and diesel engine efficiency the best torque and speed combinations is shown as functions of power in Figure 2.5.
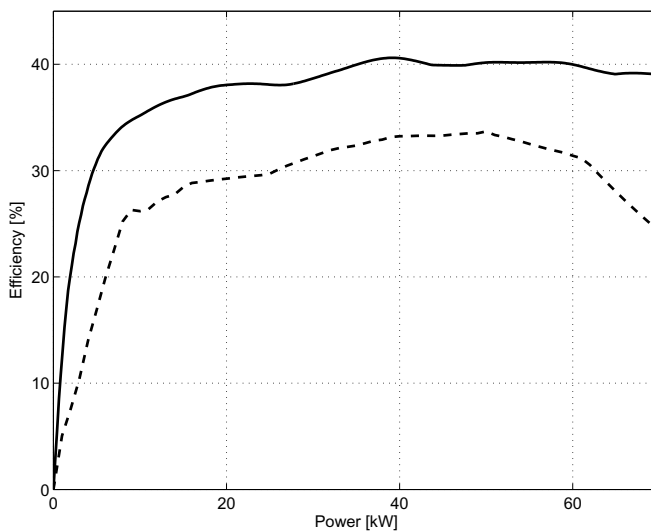
Figure 2.5:   Example of maximum efficiency for a petrol (dashed) and a diesel (solid) engine respectively.

Electric machines

In vehicle traction system electric machines utilize the interaction between electric current, magnetic field and physical geometry to create torque. Magnetic flux in all electrical machines brings two fundamental properties:

- The voltage required to run the machine is proportional, or almost proportional, to the speed of the electrical machine multiplied with the magnetic flux.

- The torque is proportional, or almost proportional, to the current supplied to the machine multiplied with the magnetic flux. This is not entirely true in the field weakening range of traction motors.

At low operating speeds the voltage requirement is correspondingly low. The torque is only limited by the limitations for the current at low speeds. This means that as long as the voltage is not a limitation, maximum constant torque can be achieved. At high speeds on the other hand, the required voltage is higher than the voltage that can be supplied. This is handled by reduction of the magnetic flux to such an extent that the product of speed and flux is slightly less than the voltage that can be supplied. This is called field weakening. See Figure 2.6.
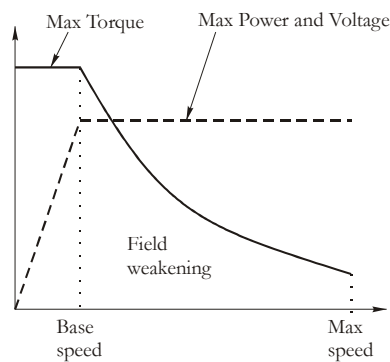
Figure 2.6:   Maximum torque in the two operating regimes of electrical machines.

When the flux is reduced, the maximum torque is also reduced since the torque is a product of flux and current. Since the flux is reduced inversely proportional to the speed as the speed increases, so does the torque too. Since power is the product of torque and speed, the power is constant in the field weakening range.

Disregarding losses, the power delivered by the electric machine can be expressed both in electrical and mechanical quantities:

$$P = speed \cdot torque = voltage \cdot current = flux \cdot speed \cdot current \qquad (2.3)$$

The traction system of an electric vehicle involves one, or several, electrical machine(s). The requirements on these machines are usually to have high torque density, i.e. the maximum torque should be high, at least at low speed. That gives good starting properties. (Alaküla, 2004, How stuff works, 2005b)

Fuel cells

Fuel cells are usually classified by the type of electrolyte they use. There are several different types of fuel cells, each using different types of chemistry. In principle it operates as an electrochemical energy storage (battery), but does not need recharging. The fuel cell operates as long as it is supplied with fuel.

A fuel cell consists of two electrodes sandwiched around an electrolyte. Oxygen passes over one electrode and hydrogen over the other, generating electricity, water and heat. See Figure 2.7 and Equation 2.4.
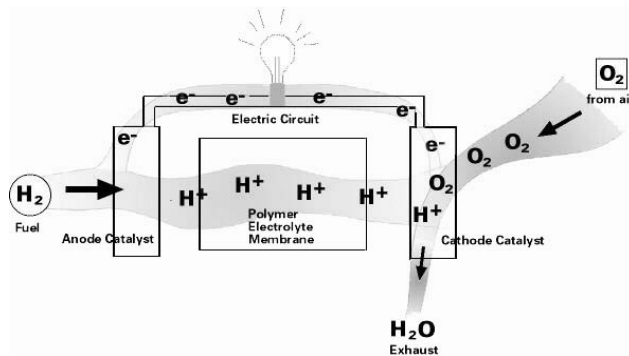
Figure 2.7:   The principle of a fuel cell.

$$2H_2 + O_2 \Rightarrow 2H_2O \qquad (2.4)$$

where H = hydrogen and O = oxygen.

A fuel cell system, which includes a "fuel reformer", can utilize the hydrogen from any hydrocarbon fuel - from natural gas to methanol, and even gasoline. Fuel cells rely on chemistry and not combustion. This means that emissions from this type of a system would still be much smaller than emissions from the cleanest fuel combustion processes. As a fact, pollution reduction is one of the primary goals of the fuel cell.

To be able to propel the vehicle the fuel cell system in a hybrid vehicle is in need of additional system components. The output voltage of the fuel cell stack varies with load. The voltage must therefore usually be conditioned to adapt to the system voltage. The same applies to secondary energy storages (e.g. battery). The electric power passes thereafter the electromechanical energy converter that finally feeds the mechanical power into the transmission system to the wheels (Alaküla, 2004 and How stuff works, 2005a).

Chapter 3

Fuel consumption and emissions

3.1 Introduction

One of the motivations for hybrid vehicles is the possibility to relatively freely choose the load point of the engine. It can of course be chosen disregarding the effects of the fuel consumption and emissions and only regarding the car performance and driveability.

This study is made with the intention to reduce the fuel consumption and to fulfil the future intended NO_X emission regulations, with maintained possibility to carry out overtaking without intimidating the fellow passenger or the fellow road-users. That implies a sufficiently large engine for overtaking with the side effect of sometimes being too large.

In the following sections the motives, claims and causes that constitute the foundation of the actions taken in this study will be presented.

3.2 Fuel consumption

For a vehicle, especially a heavy vehicle operating in traffic, the purchase price is by far surpassed by the operating expenses. The fuel consumption is one of the main items among the operating expenses.

The average customer is anxious about keeping the fuel expenses as low as possible. All future prospects point at a continuously increasing price on fuels.

The fuel consumption is depending on the ICE speed and torque demand. The fuel consumption is also depending on engine design, aerodynamic design, drive cycle, driver behaviour, fuel energy contents etc.

The vehicle weight has an important impact. There is a method available to calculate the effect that a revised vehicle design will have on the fuel consumption. From a general point of view 50 kg extra vehicle weight is equivalent to 100 W losses for a standard passenger car (Miller – Nicastri, 1998).

Power is equal to a certain combination of torque (T) and speed (ω). Hence follows that different torque and speed combinations can supply a certain power. This is however done with different ICE efficiency. The T / ω characteristic of a petrol engine is shown in Figure 3.1.
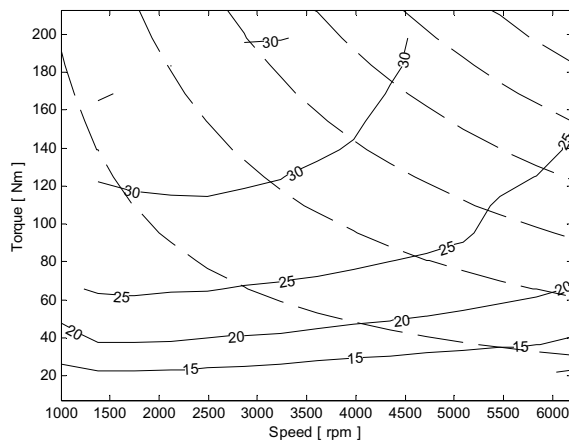
Figure 3.1:   Example of efficiency diagram for a petrol engine. The ISO lines (dashed) indicate where different torque and speed combinations will supply a certain power.

3.3 Emissions

The environmental impact of the use of a vehicle is an interesting variable. The emissions are not linearly dependent on fuel consumption or mileage. The construction of machinery, in connection with vehicle design, control methods, drive cycle, driver behaviour, choice of fuel etc are together defining the total emissions. Last but not least, the emissions are affecting the environment, through green house gases and toxic pollution, from the very first emitted mass.

At combustion of fossil hydrocarbons, several emissions will be formed. Only the regulated emissions will be dealt with below.

Complete combustion means that all hydrocarbons (HC) are transformed into carbon dioxide (CO_2) and water (H_2O). This is called stoichiometric combustion. $(A/F)_S$ is the stoichiometric air (A) to fuel (F) mixture, i.e. the mixture with minimum air supply that theoretically could lead to complete combustion. The ratio between the amount of actual and stoichiometric fuel-to-air mixture is better known as λ, defined in Equation 3.1.

$$\lambda = \frac{\left(\dfrac{A}{F}\right)_{actual}}{\left(\dfrac{A}{F}\right)_{s}} \qquad (3.1)$$

When $\lambda < 1$, all fuel is not transformed properly into CO_2 and H_2O and unwanted emissions occur. This happens for instance at fast accelerations, when the power demands changes.

Some emissions are governed by legislative regulations and some are not. Hydrocarbon (HC), carbon monoxide (CO), nitrogen oxide (NO_X) and particle matters (PM) are included in the regulated ones. Among the unregulated residuals there are formaldehyde and polyaromatic hydrocarbons. The emissions will be dealt with in next section.

In a HEV, using an otto engine, it is possible to achieve $\lambda = 1$ by choosing a control law that uses the electric machines for transient power demand. The ICE is therefore controllable and neither too little nor too much oxygen is available at fuel combustion. (Andersson et al., 2000a, Johansson, 1999, Bäckström, 2000, Heywood, 1988) A good popular description can be found in (How stuff works, 2001b).

When measuring emissions, it is important to keep in mind that the result can vary between two measurement occasions with the same conditions. One reason is the temperature, both the outdoor temperature, but also the temperature of the engine. The measuring methods are another cause. Hereby is it wise to handle the absolute emission figures with care. Using the measured emission results in simulation models as an instrument for relative comparison, where the mutual order of magnitude is in focus, is on the other hand not suffering from possible sources of errors to the same extent. When studying the simulation results it is rather the relative change of emissions then the absolute figures that should be emphasized.

The emissions in this survey are specified in g/km. The emissions during a drive cycle are accumulated and a mean value for the cycle is created. By using an average value instead of the sum of emissions from a cycle, is it possible to compare cycles with different length.

Nitrogen oxides and particle matters

Oxygen and nitrogen in the air react at high temperatures at combustion (>1800 K) and forms NO_X. The NO_X reacts with water and causes acid rain, which is detrimental to the environment. It also causes choking and can cause cancer (Andersson et al., 2000a and Papadakis, 2003).

The dominating and, not negligible, drawback with especially the diesel engine is the NO_X emission and particulates. The emissions and particulates are depending on the chosen control strategy and are hereby possible to affect to some extent. There is however some environmental benefits of diesels, such as low greenhouse gas emissions.

U.S. Environmental Protection Agency claimed 1999 34% of the nitrogen oxides in USA to derive from on road mobile sources. Of these 47% are from diesel vehicles (e.g. 16% of the total amount) (U.S. Environmental Protection Agency, 2005a).

Particulate Matter (PM) it the term for solid, or liquid, particles found in the air. Soot or smoke is PM that is dark or large enough to be seen with the naked eye. Generally PM originating from mobile sources is too tiny to be visible, since they are less than 2.5 microns in diameter.

U.S. Environmental Protection Agency claimed 1999 10% of the PM in USA to derive from on road mobile sources. Of these 72% are from diesel

vehicles (e.g. 7% of the total amount). (U.S. Environmental Protection Agency, 2005b)

Hydrocarbons

At combustion with a deficiency or surplus of oxygen incomplete combustion causes HC to be formed. The hydrocarbons are poisonous to human and can cause cancer.

U.S. Environmental Protection Agency claimed 1999 29% of the hydrocarbons in USA to derive from on road mobile sources. Of these are 5% from diesel engine (e.g. 1% of the total amount). (U.S. Environmental Protection Agency, 2005c)

Carbon monoxide

CO is formed at imperfect combustion from CH to CO_2 with a deficiency of oxygen or at uneven fuel mixture. CO blocks the ability to absorb oxygen.

U.S. Environmental Protection Agency claimed 1999 51% of the hydrocarbons in USA to derive from on road mobile sources. Of these are 4% from diesel engine (e.g. 2% of the total amount). (U.S. Environmental Protection Agency, 2005d)

3.4 Regulations and legal constrains

The damage of the green house gases, toxic pollutions etc are priceless. Even though there are price labels possible to use and their correctness can be questioned. Authorities have their opinion of the "price" of emissions and by introducing taxes they endeavour to reduce the emergence of emissions.

The taxes are often used as a control instrument and are influenced by the occurrence in the world around, i.e. international environment agreements. The tax levels are not an easily defined function of the environmental impact.

As a result of taxes, emission quota assigned to companies by authorities, and penalty fees when the outlet figures are exceeded, a market for CO_2 emission quota has arisen. This brings about another emission price,

assigned by the market and fluctuating as like stock-exchange prices (Emissionstrading, 2002).

The European Union has regulations for vehicle emissions and the Directive 70/220/EEC specifies the one used for new light duty vehicles. The directive has been amended several times, and is specified in Euro 1, Euro 2, Euro 3/4. There are plans for Euro 5 for passenger cars, but the extents of these regulations are not stipulated yet (see Table 1). Euro 3 and 4 include more stringent fuel quality rules[3]. The emissions are tested over the ECE+EUDC cycle (see Figure 5.11). All emissions are expressed in g/km. (Dieselnet, 2004b and European Union, 2005)

Table 1: Extract from EU Emission Standards for Passenger Diesel Cars (Category M), [g/km].

Parameter:	Introduction year:	NO$_X$:	PM:
Euro 1	1992	-	0.14
Euro 2	1996	-	0.08 [4]
Euro 3	2000	0.50	0.05
Euro 4	2005	0.25	0.025
Euro 5[5]	not stipulated	outline: 0.08	outline: 0.0025

In the preliminary works with Euro 5 an initial questionnaire was distributed in the beginning of 2004. The results of this questionnaire are being summarized at the time of writing. The NO$_X$ emission levels for diesel passenger cars discussed in this questionnaire are 0.075 - 0.15 g/km. (Weissenberg, 2004)

---

[3] Euro 3 and Euro 4 also regulate required minimum diesel cetane number, maximum diesel sulphur content as well as maximum petrol sulphur content.

[4] 0.10 g/km during the period 1996-01-01 -- 09-30.

[5] German proposal for Euro 5. (European Union, 2005)

3.5 Emission control

Catalyst

Mostly vehicles using an otto engine are today equipped with a three-way catalytic converter (TWC) to reduce the emission. The TWC is coated on the inside with a precious metal that causes the CO to convert to CO_2 and the HC into CO_2 and water. Furthermore the TWC converts the NO_X back to N_2 and O_2.

The volume of the TWC is of the same order of magnitude as the displacement of the engine. Since the surface is equipped with a structure like honeycombs that is covered with a wash-coat, the active surface can reach $10000m^2$. The large area is necessary to make it possible for the emissions to be exposed to the precious metals during the passage through the TWC. (Johansson, 1999)

The active layer in the TWC is sensitive for lead, and therefore an engine equipped with a TWC must be run with unleaded fuel exclusively. Lead in a TWC forms a coat that blocks the precious metals.

The conversion rate of the TWC is temperature dependent. No efficient activity takes place at a temperature below 250°C. Ideal working conditions takes place at temperatures of 400 – 800°C. Too high running temperature can damage the catalyst as well. The precious metals run the risk of melting together. This implies a decreased active layer. (Bosch, 1996 and Johansson, 1999)

This emission reduction is strongly dependent on the λ value. There is only a small λ–window where this works. Figure 3.2 shows the variations of HC, CO and NO_X before TWC and Figure 3.3 shows the emission after reduction in the catalyst (Heywood, 1988). Note the small λ-window, i.e. the space at $\lambda = 1$ where there is a emission minimum for all three emissions at the same time. The exact shapes of the graphs are depending on the engine configuration.
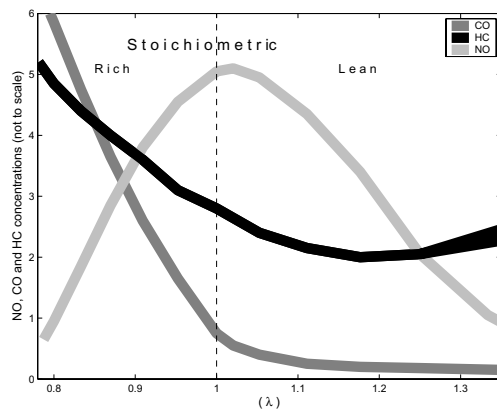
Figure 3.2:   The figure shows the variation of HC, CO and NO concentration in the exhaust of a conventional spark-ignition engine with air/fuel equivalence ratio.
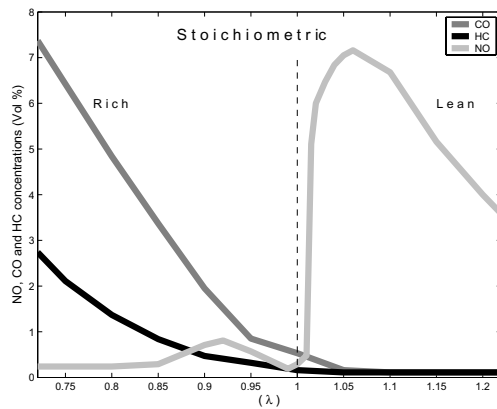
Figure 3.3:   Remaining emissions after a three-way catalyst.

At fast acceleration, the power demand changes rapidly and possibly forces the λ value outside the λ-window, if the TWC-control algorithm is too slow.

Exhaust gas recirculation

Formation of NO_X is strongly depending on the temperature in the combustion chamber. By diluting the reaction mixture the temperature can be reduced and the NO_X formation will decrease. The exhaust gases are

used for this purpose. Some of the heat in the chamber will then be used to heat the inert gas, and the result is a lowered maximum temperature in the combustion chamber. This procedure is called Exhaust Gas Recirculation (EGR) and circulates exhaust gas back to the air intake manifold (Heywood, 1988 and Jonasson, 2003).

A common disadvantage to EGR systems is the susceptibility to clogging of valves and plumbing, caused by exhaust deposit. This clogging results in gradual reduction in recirculation rates in course of time (Bosch, 1996).

Selective catalytic reduction

There are other alternative solutions available for reducing the NO_X emissions, for example Selective Catalytic Reduction (SCR). A nitrogen-reducing compound, such as urea or ammonium, is injected in the exhaust gas. This is done in proportion of present NO_X. (Chevron, 2003 and Jonasson, 2003) Research has also been done of injecting diesel into the exhaust gases, which results in decreased NO_X, but also increased fuel consumption (Künkel, 2001).

Chapter 4

Controlling electric hybrid systems

4.1 Criteria

Before being able to decide what is the best, or at least what is a good, choice, we need to state what is "good". There is also a need to clarify why certain criteria have been chosen and others have not. Some criteria are imperative, like legislations, others are subjective, like ride comfort. Yet others are depending on location and/or political decisions and there are, in the end, criteria that are easy to measure and hereby less debateable.

In this study the focus for valuing the performance of the hybrids are chosen to be the fuel consumption and the NO_X emissions. These are both measurable quantities, well known and of significance for the customers, the environment and thus the decision-makers.

Fuel consumption

The fuel consumption is depending on engine design, aerodynamic design, vehicle weight, drive cycle, driver behaviour etc. The largest variable cost is, for most vehicle owners, the fuel consumption. Therefore it is a frequently asked question from consumers in connection with evaluation of a car's performance. In a wider perspective it is of interest since the oil resources are limited and it is therefore of great importance to global economy.

Nitrogen oxides

The high efficiency of the diesel engine is something the hybrid can take advantage of. But the diesel engine has a heavy drawback, the NO_X emissions. It is therefore important to focus the efforts on reducing these emissions and actions are taken in this study to achieve exactly that. The means for NO_X reduction, used in this study, are to control when and how the ICE is used, use emission control and add exhaust-gas aftertreatment.

4.2 Means

There are many degrees of freedom for the control of a hybrid electric vehicle. Some of the parameters are related to design and others are related to operating parameters. This implies many adjustable parameters in the simulation model; vehicle chassis parameters, combustion engine, electric machine(s) and battery size and types, losses models, charging strategies and driver behaviour etc. To investigate all of them is possibly interesting but not realistic in this study. It is not the aim and the result flow would be overwhelming. This study has chosen to focus on a limited number of control possibilities. The aims have been to reduce fuel consumption and to fulfil the future intended NO_X emission regulations. The control parameters used in this study will be presented in this chapter.

Control strategy

The presence of a secondary power unit, primary and/or secondary energy storages in the vehicle creates unique control possibilities for the hybrid vehicle compared with the conventional vehicle. By using a control algorithm that avoids the disadvantage and benefits the advantage, a new dimension in vehicle control is obtained.

Time constant, τ_{ICE}

A fundamental consideration when dealing with hybrid electric vehicles is that the dynamic operation of the ICE must be limited. It is argued that an ICE consumes fuel and generates emissions out of proportion when making changes of operating point with a certain rate, compared to the fuel consumption and emissions in stationary operation (Andersson, 2001).

The simplest way to limit the dynamic operation of the ICE is to low pass filter the required power from the ICE. See Figure 4.1. The choice of time

constant therefore significantly affects the vehicle behaviour and must be selected to ensure quasi-stationary operation of the ICE.
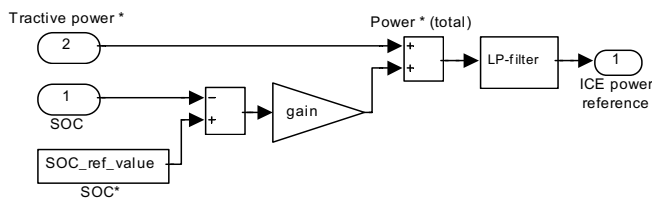

Figure 4.1:   A generalized view of the part of the power distribution block in the simulation models that handles the calculation of ICE power reference.

With τ_{ICE} theoretically set to zero, the engine is used like a engine in a conventional vehicle. No power is supplied from the battery, if the ICE can deliver the demanded power. The drawback is that a transient behaviour of the ICE involves an increased amount of emissions. When τ_{ICE} increases, the battery has to supply an increased amount of transient power.

Charging gain, K_{Pice}

The ICE power demanded is a sum of power demands for traction, auxiliary power (not shown in Figure 4.1) and a proportion of the deviation of the SOC. See Figure 4.1. When the SOC diverges from its reference value, a *P*-controller requests a correction (the battery can be overcharged as well). With a small gain factor, a SOC deviation is slowly corrected, i.e. the battery is permitted to compensate for a transient ICE power request. This will be done to the price of larger deviations of SOC. A larger gain factor adjusts the SOC deviation quicker, at the expense of higher ICE power and its associated emissions.

The SOC deviation is multiplied with both the maximal ICE power and with a gain factor, called K_{Pice}, and thereafter added to the total ICE power demand. When choosing a larger gain it is accompanied with reduced utilization of the battery. The ICE has to supply the power demand on its own to an increasing extent when the gain is increased. A small gain stresses instead the battery. A large deviation in SOC reduces the battery lifetime and consequently ought to be avoided.

The charge control algorithm suggested in Figure 4.1 is simple, and more advanced methods are proposed in literature (Rutquist et al., 2004). It is however rather efficient when compared to much more ambitious

algorithms (Hellgren, 2004). Since the focus in this thesis is on control aspects related to the ICE itself, no study deeper that the one already presented in (Jonasson, 2002) is made here.

Efficiency optimization

To achieve a certain demanded power there are several feasible torque/speed combinations (load points). The different load points will though imply different efficiencies. One of the advantages with hybrid vehicles is that the engine speed can be chosen relatively freely relative the vehicle speed. It is, after all, depending on transmission (6-speed manual-, 6-speed automatic transmission or CVT). Therefore an examination of the efficiency for all possible load points, for every single power level in the engine in question, has been made. The aim is to guarantee the highest possible efficiency for the present power demand. This has been carried out as follows: An optimization algorithm will find a number of load points with optimum efficiency. These points are not necessarily connected along a smooth path, but represent the best efficiency for each power value. In order to obtain a system where the engine can change its load point smoothly during a driving cycle, the various optimum load points have been connected along a smoothened path. This path represents the most efficient operation for different power values. The result is shown in Figure 4.2.
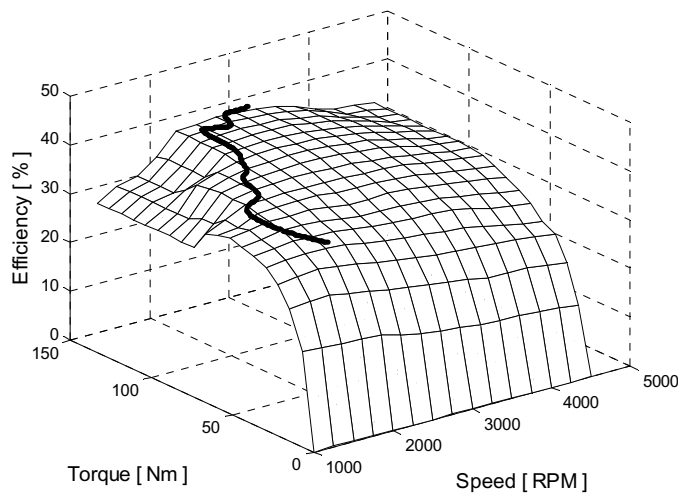
Figure 4.2: Optimal choice of load point considering the ICE efficiency for the diesel engine in the simulation model.

This data is then used in the simulation model, as an imperative choice of engine load points, though considerations regarding the gears have to be taken.

Note in Figure 4.3, showing the optimal choice of load points when optimizing for lowest NO_X, that there is a small "dent" in the efficiency map at around 2750 rpm and 70 Nm. This is the centre of the region where the EGR is active, and the negative effect on the efficiency of the EGR is clearly visible. Simultaneously, the NO_X map in Figure 4.4 shows that the EGR is efficient on NO_X reduction. This observation hints that optimisation of the choice of load-point at least is a compromise between efficiency and emissions.

Nitrogen oxide optimization

Since the highest possible efficiency to some extent also coincides with the maximum value for NO_X emissions, there are reasons to consider an alternative strategy regarding choice of operating point. Therefore the same procedure, as to appoint the maximum efficiency, has been carried out to map the minimum NO_X-path for varying power demand. See Figure 4.3.
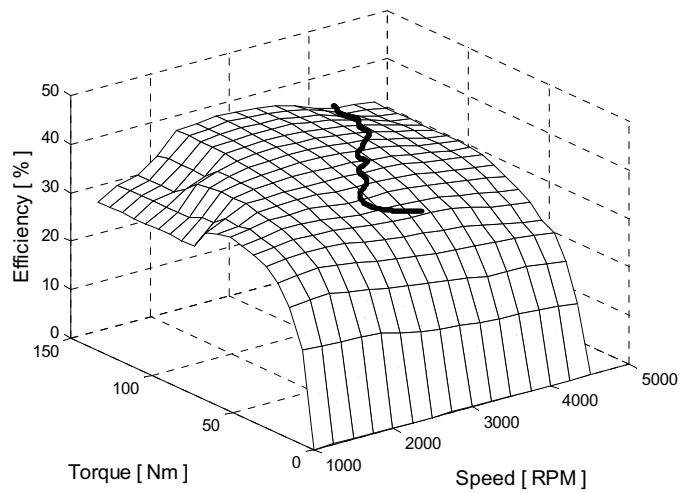
Figure 4.3:   Optimal choice of load points considering the NO_X production for the
engine in the simulation model.

The different results in NO_X productions are visualised in Figure 4.4 where
the NO_X emissions and the load point choices are shown.
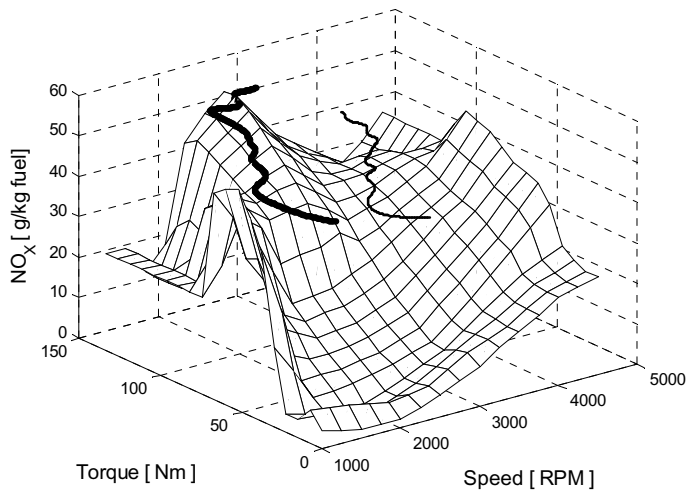
Figure 4.4: NO_X emission when choosing load point considering the ICE efficiency (thick line) and the NO_X emissions (thin line) respectively for the engine in the simulation model.

Gear ratio and gear shift control

Yet another control parameter is the choice of gearbox, its gearing and its final drive ratio. Should the vehicle be equipped with a 5- or 6-speed manual or automatic transmission or a CVT? The choice of transition speeds/levels between different gears in a X-speed gearbox represents yet another degree of freedom.

To investigate the impact of different gear ratios different solutions have been implemented in the simulation model. Besides the gear ratios, belonging to the vehicle where the engine derives from, some alternative gear ratios have been defined. The gear transition levels have also been adapted for lowest fuel consumption or lowest NO_X emission.

Figure 4.5 shows two examples of gearshift strategies, one CVT and one 6-speed gearbox.
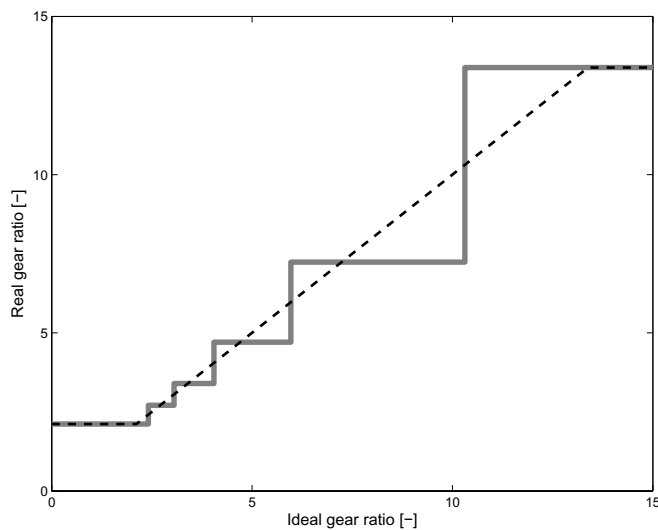
Figure 4.5:   Gearshift strategies. CVT strategy (dashed black line) and 6-speed
gearbox (solid grey line).

Cylinder deactivation

The main advantage with a hybrid vehicle is the possibility to choose to
only operate the ICE when the efficiency is above a certain limit. This
results in electric mode at low velocity. Inversely it implies that a
conventional vehicle operates at low efficiency when driving in city traffic.
One way of rectifying this would be to equip the conventional vehicle with
a smaller engine. But that results in a vehicle that cannot keep up with the
highway speed or manage swift overtaking.

A solution to this issue is to use cylinder deactivation, i.e. to switch off a
certain number of cylinders at low power demand. If hybridization and
cylinder deactivation are combined, new possibilities open up. The working
area representing the sufficiently high efficiency would increase in other
words. The solution also benefits the conventional vehicle.

The number of deactivated cylinders can, theoretically, vary from zero to
all, except one, of the present cylinders. In this study the efforts have been
focused on full sized engine and an engine with half of the cylinders
deactivated.

Deactivating the engine implies that consideration must be taken to the deactivated cylinders. The cylinders cannot just be "switched off", unless the engine does not actually consist of two engines, where one can be switched off. The drawback with that solution is the need for mechanic separation of crankshaft, camshafts etc.

When the cylinders are not switched of, but deactivated, it implies that the pistons are moving up and down without combustion taking place. The fuel feed is interrupted as well as the ignition. The movement of the pistons is taking place due to the existence of a common crankshaft. The movement of the deactivated pistons however, still suffer from mechanical losses.

If decoupling of cylinders is not possible, the optimum cylinder deactivation would be to close valves and fuel feed for the deactivated cylinders. This would however require a flexible valve mechanism.

The piston movement in a conventional engine implies that gas exchange is taking place. This brings about that air from the deactivated cylinders will be diluting the exhausts from the other cylinders, cooling down the exhaust gas mixture. It also results in pump losses and a risk that the catalyst becomes to cold.

The power extracted in the burning fuel should not only propel the vehicle, it should also overcome the inner losses of the engine, the friction losses. These inner losses are, for example, piston assembly, pump losses, compression losses, valve train, crankshaft and seals. Their relative impacts vary depending on engine speed.

If the engine were equipped with a valve mechanism without a common camshaft, which makes it possible to control the valves individually, it would open up a possibility to reduce the losses from the deactivated cylinders. Such technology is currently being evaluated by the automotive industry and may very well be a reality in a not to distant future.

A common way of describing the conditions of the loading of the engine is to measure the pressure in the cylinder during the four strokes. The Indicated Mean Effective Pressure (IMEP) is calculated as follows (Heywood, 1998):

$$IMEP = \frac{\oint p \, dV}{V_D} \qquad (4.1)$$

where IMEP = [Pa], p = cylinder pressure [Pa], dV = volume change [m^3] and V_D = piston displacement [m^3].

A mean pressure can also be calculated by means of the load of the engine shaft. The Break Mean Effective Pressure (BMEP) for a four-stroke engine is calculated as follows (Heywood, 1998):

$$BMEP = \frac{4\pi T}{V_D} \qquad (4.2)$$

where BMEP = [Pa] and T = torque [Nm].

The difference between IMEP and BMEP describes the total mechanical losses of the engine, described as a mean pressure. This Friction Mean Effective Pressure (FMEP [Pa]) can be expressed as (Heywood, 1988):

$$FMEP = IMEP - BMEP = f(enginespeed) \qquad (4.3)$$

The speed dependency of FMEP can be seen in Figure 4.6.
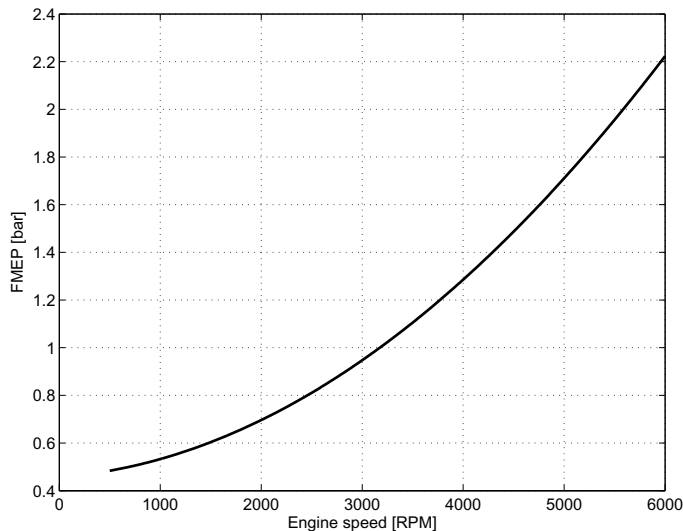

Figure 4.6:   Total FMEP (total mechanical losses in the engine) vs. engine speed.

The losses, FMEP, are depending on what is connected to the shaft. The normal is to consider that only the loads necessary for the engine function are connected, such as valve mechanism, injection-, water- and oil pumps.

To these losses should also the inner losses of the engine, such as gas exchange losses and frictions, be added. This means that FMEP consists of a sum of mean pressures (friction, gas exchange and attachments).

When simulating the engine with deactivated cylinders, the losses caused by the deactivated cylinders have been considered as an added load. This means that efficiency and emission characteristics will be retained for a single load point defined by BMEP and engine speed. Scaled engine data will constitute a simple, but satisfactory, description of the engine running with deactivated cylinders. The active cylinders propel the deactivated cylinders and make up for their losses. The extra load that the deactivated cylinders cause can be calculated by means of the displacement for the deactivated cylinders and FMEP.

This simplification is however not completely true, since compression of the enclosed charge causes heat that will be transferred to the walls. This leads to that some of the compression works would not be retrieved during the expansion stroke. This approximation does not take these cooling losses into consideration.

The diesel engine used in the simulation is equipped with a turbocharger. It is assumed that the turbine is provided with an adjustable inlet nozzle to be operated depending on whether some of the cylinders are deactivated or not.

Further references can be found in (Challen, 1999, Heywood, 1998, Stone 1999 and Taylor 1982).

In Figure 4.7 the efficiencies for the engine used in the simulation model and the same engine with deactivated cylinders are shown. The gain of the reduced engine size is clearly visible at and around the area of 75 Nm / 2500 rpm. The friction losses (FMEP for the deactivated cylinders) result in reduced efficiency and they are clearly visible at high speed for the deactivated engine, which also can be seen in Figure 4.7.
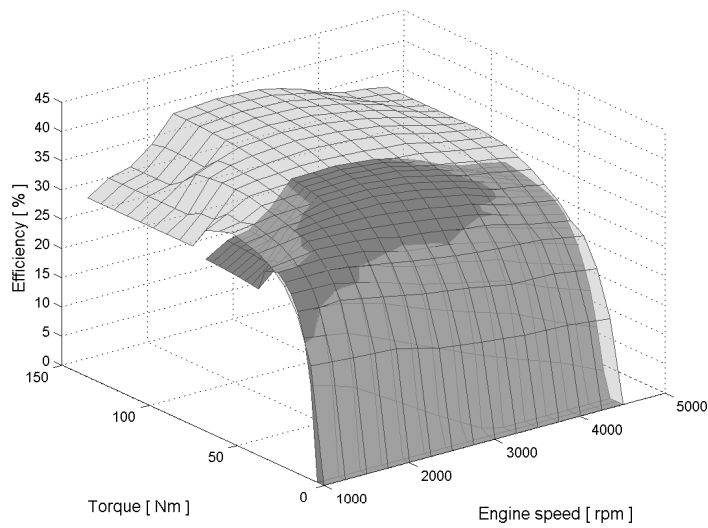
Figure 4.7:   Engine efficiency when running as full sized engine (brighter) and with
half of the numbers of cylinders deactivated (darker) for the diesel engine
in the simulation model. Note the increased efficiency that the
deactivated engine implies in the area of 75 Nm / 2500 rpm compared to
the original engine size.

Figure 4.8 describes the highest possible efficiency of the engine in question at different power levels. The speed dependency of the losses is visible at high speed for the deactivated engine. The gained efficiency at low power is also easy visible.
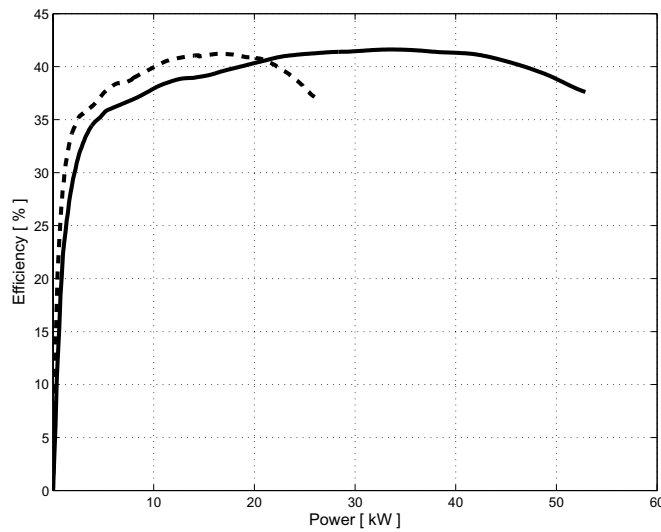
Figure 4.8: The figure shows the highest possible ICE efficiency for full size (solid line) and deactivated engine (half of the number of cylinders are deactivated, dotted line) The ICE efficiency losses is visible for example at efficiency peak level and at highest possible power, where the deactivated engine show lower ICE efficiency than the original engine. The advantage of the deactivated engine is visible at power below 20 kW.

Exhaust gas recirculation

Exhaust Gas Recirculation (EGR) in an engine for a conventional vehicle does not suit the engine in a hybrid application, since the load point where the EGR is used does not necessarily coincide with the load points preferred in the hybrid application. A purpose of a hybrid vehicle is to achieve a higher efficiency than a conventional vehicle uses. The best efficiency is reached at load points different from those where the EGR is in operation in a conventional vehicle. Therefore it needs an adjustment for hybrid application (Jonasson, 2003).

To stress the maximum possibilities that EGR supplies with, the highest used EGR has been detected in the data belonging to the engine in question. A new efficiency and NO_X map has then been created, with the highest used EGR all over the working area. This is a method to investigate the possibilities an adjusted EGR could bring about regarding NO_X emission

and efficiency. In Figure 4.9 the original and the adjusted EGR map are shown (scaled to the engine size used in the simulation model).
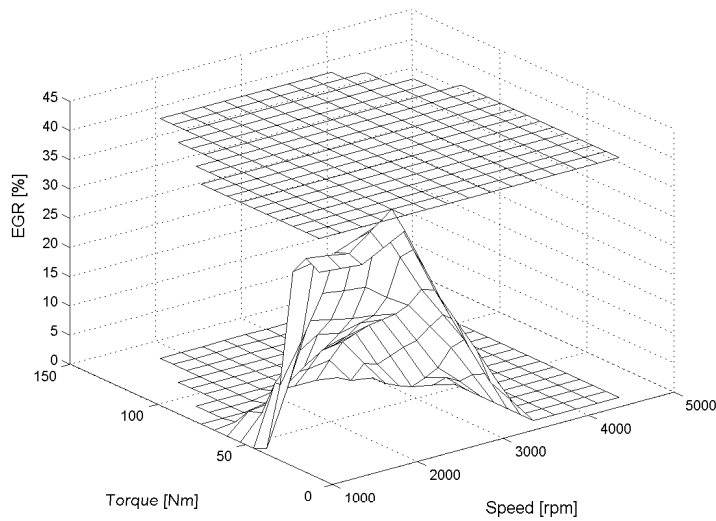
Figure 4.9: The figure shows the original EGR (lower graph) and the adjusted EGR (upper graph). Since the hybrid vehicle is controlled to use high ICE efficiency, the working area ends at an area mainly outside the peak of the original EGR.

The impact of the EGR on NO_X is determined. As foundations of this a black box model has been used. See Figure 4.10. The purpose of this model is to determine if it is possible to find a correlation between engine speed, torque, EGR and NO_X emissions.
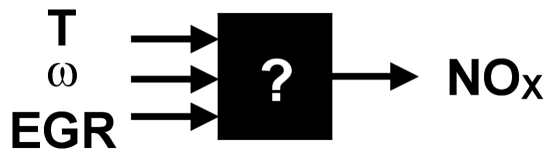
Figure 4.10: The black box model describing the correlation between torque, engine speed and emission that is searched for.

A number of empirical structures have been tried to capture the relationship. It is true that there is a significant non-linear relationship

between the NO_X and the three inputs. Furthermore it is assumed that the relation is static. It turned out that the following equation fulfil the expectations:

$$NO_X = A * N^B * T^C * \exp\left(D * \frac{EGR}{100}\right)$$ (4.4)

where *A*, *B*, *C* and *D* are constants (see Table 2), *N* = engine speed [rpm] and *T* = torque [Nm].

The parameters of Equation 4.4 are determined by means of the toolbox *Non Linear Regression Tool* in the statistical program package SPSS. In Table 2 the result from the determination of the parameters *A - D* and the 95% confidence intervals are shown.

Table 2: Result from the calculations of parameters in the black-box model shown in Figure 4.10.

Parameter:	Estimate:
A	0.0008
B	0.82
C	1.19
D	-3.27

The result is shown in Figure 4.11. The obtained correlation has been used to adjust the existing data to correspond to the increased EGR usage, or, better explained the parameters estimation is used to determine the relative influence on NO_X emissions of increased EGR.
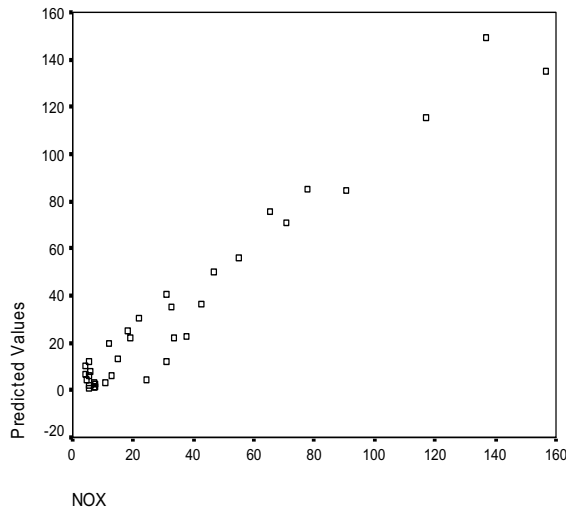
Figure 4.11:   Predicted NO$_X$ (y-axis) and outcome (x-axis). The unanimity of the existing data with the calculated values is shown in the graph. The calculations are based upon the black box model shown above.

The EGR cannot just be increased without consequences. Raising the EGR leads to efficiency losses. To determine these losses, results from measurements have been extrapolated. These measurements were carried out on single cylinder direct injected diesel engine with the specification shown in Table 3. All tests were performed at full load 1200 rpm, in the working space 0-15% EGR (Egnell, 2001).

Table 3: Test engine specification (Egnell, 2001).

Bore/Stroke [mm]	127/154
Displacement [dm^3]	2.0
Compression ratio [-]	18
Swirl ratio [-]	2.0
Injection system	Unit injector

Initial calculations concerning the impact of increased EGR on the efficiency is carried out. These calculations are based on a similar black box model as shown in Figure 4.10, but for torque, engine speed, EGR and efficiency. The model resulted in negligible influence caused by EGR on the engine efficiency.

The results received from the extrapolated measurements (Egnell, 2001) are larger than preliminary calculations of efficiency losses caused by enlarged EGR map. The extrapolated experimental data has nevertheless been used. The error will hereby rather be overestimated, than underestimated, i.e. the efficiency is most likely to low in the used model. In Figure 4.12 the losses caused by increased EGR is shown (Egnell, 2001). The results are then normalized and the relative change of EGR is used to determine the efficiency loss.
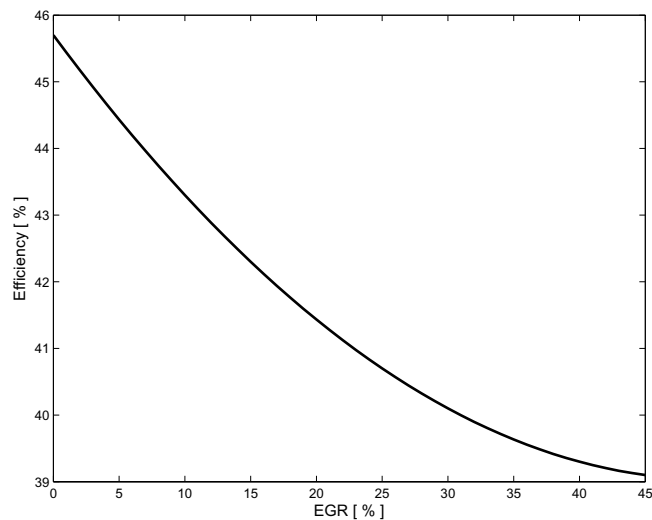
Figure 4.12: The ICE efficiency losses caused by increasing EGR. Extrapolated test results made at full load, 1200 rpm (Egnell, 2001).

The increased EGR influences the efficiency negatively. The impact is clearly visible in Figure 4.13. The original EGR map has no EGR at all load points. Since one of the main purposes with hybrid vehicles is to achieve highest possible efficiency, this resulted in low or no EGR if a conventional EGR control was used in a hybrid vehicle. Figure 4.13 clearly visualizes the impact and its efficiency loss. The reduced NO_X emissions can bee seen in Figure 4.14.
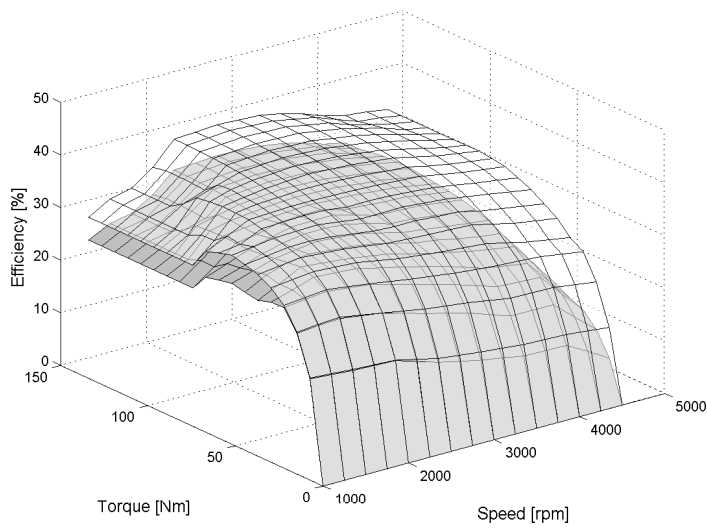
Figure 4.13:   The ICE efficiency with original EGR (white) and with increased EGR (grey). Note that the losses increase at high torque. EGR where low or non-existent previous in those regions.
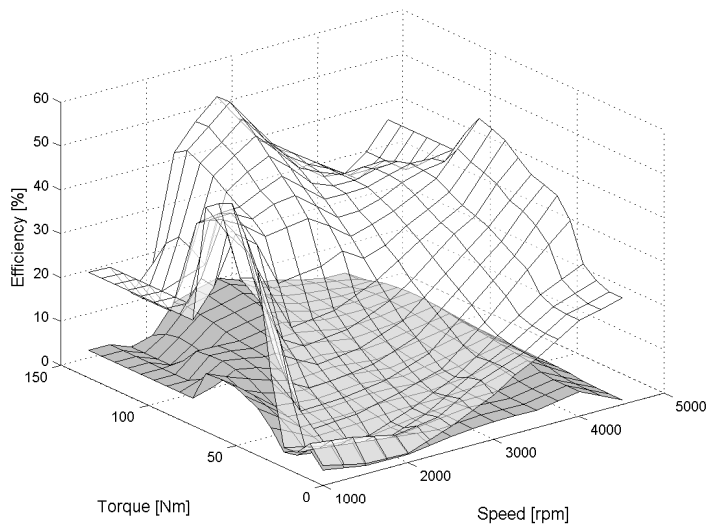
Figure 4.14:   The figure shows NO_X emission with original EGR (white) and NO_X emission with enlarged EGR (grey).

Selective catalytic reduction

The aim with Selective Catalytic Reduction (SCR) is to reduce the NO_X emissions in the exhausts, by means of adding urea. To be precise it aims to reduce NO_X by means of reduction of NH_3 (in urea) to N_2 and H_2O.

$$NO + 0.25\,O_2 + NH_3 \rightarrow N_2 + 1.5\,H_2O \qquad (4.5)$$
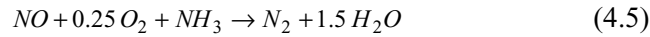
This equation denotes a combined oxidation and reduction process. The degree of NO_X reduction is depending on the exhaust temperature that in its turn is depending on the chosen load point. The influence of the temperature is shown in Figure 4.15 (Andersson et al., 1994). The measurements are made at 1200-1800 rpm in stationary pilot experiments on a 3.6 dm^3 engine. That does not correspond to the range of revolutions the engine in question works at. The engine speed is not the dimensioning factor of the catalyst, but the flow through the catalyst is. The simulated catalyst is therefore chosen to correspond to the flow of the simulated engine.
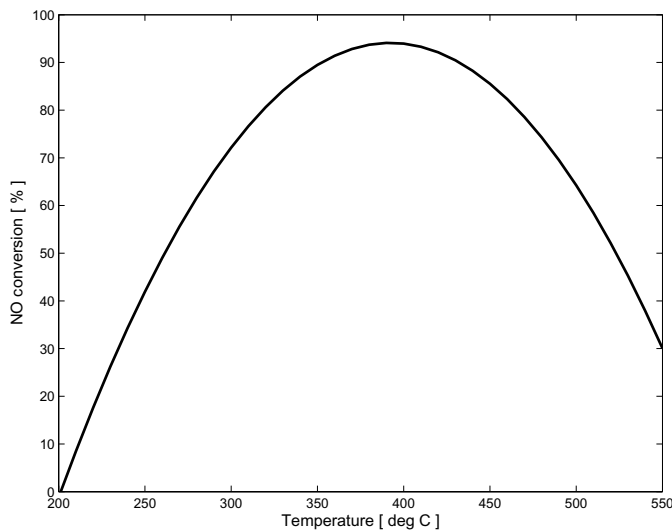
Figure 4.15:   The graph shows an approximation made from experiments on NO_X conversion vs. temperature.

When implementing SCR in the simulation model, the model is based on experimental data. This data originates from stationary experiments on a 3.6-dm^3 engine with a 4.8-dm^3-honeycomb catalyst (Andersson et al.,

1994). One mole urea corresponds to two moles ammonia, which reduces 2 moles of NO. The product that is used is called Adblue and contains 10% urea and 90% water (Odenbrand, 2004). The price of Adblue is 7.5 SeK/l and includes 25% VAT (International Diesel Service, 2005).

When running the engine in hybrid application it implies usage of the ICE at high efficiency, i.e. at high temperature. As can be seen in Figure 4.15 the SCR efficiency increases at high temperatures. This makes the hybrid vehicle particularly suitable for implementation of SCR.

The exhaust temperatures used in the simulation model derive from to the same diesel engine, where efficiency and NO_X emission data originate from. A change in temperature might result in either decreased or increased conversion efficiency of SCR catalyst. See Figure 4.15. The influence of SCR on the NO_X formation can be seen in Figure 4.16.

The option of increased EGR in combination with SCR has also been examined. The altered NO_X emission data is shown in Figure 4.17. These data do not take the changes in exhaust temperature caused by the EGR into consideration. Measurements presented in (Egnell, 2001) shows that implementation of EGR causes increased exhaust temperatures. Since the exhaust temperature in the simulations appears in the range 250-400 °C, an increased temperature would rather increase the NO_X conversion. This means that the potential of SCR rather is underestimated than overestimated.
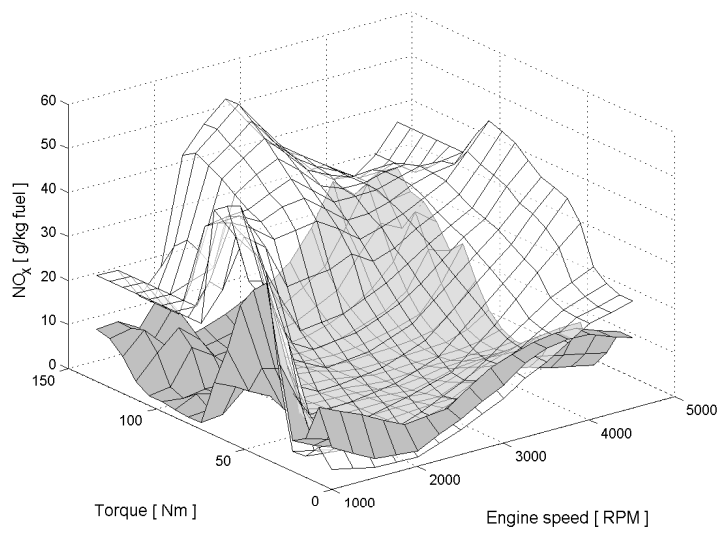
Figure 4.16:   The graph shows original NO_X emission (white) and NO_X emission after SCR is applied (grey).
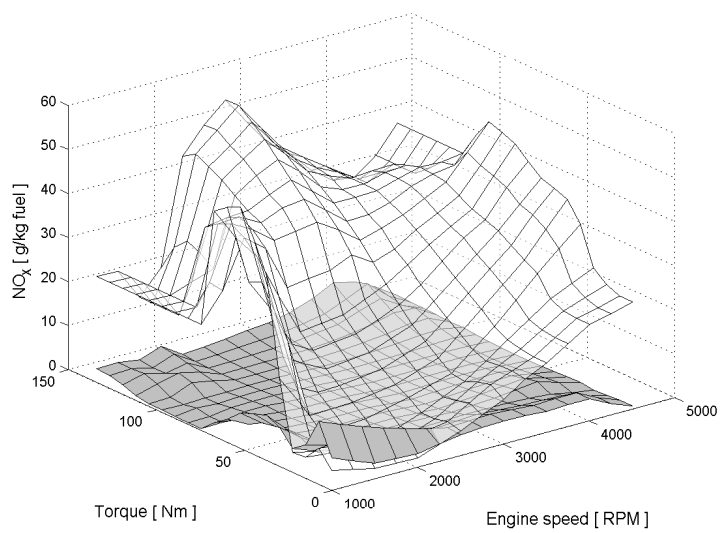
Figure 4.17:   The graph shows original NO_X emission (white) and NO_X emission after both SCR and enlarged EGR is applied (grey).

Chapter 5

Simulation model

To model a HEV system is quite a complex task. The dynamics are varying from less than µs in the power electronics to long-term effects of wear and ageing. It is necessary to limit the modelled dynamics with regard to the purpose of the simulations.

There are several software environments suitable for analysing such systems. For this task the Matlab®/Simulink® environment has been used. It is a widely spread simulation program both in industry and in academia. This study is a continuation of the results, produced in previous studies (Jonasson, 2002) and (Strandh, 2002), which also were carried out in Simulink®.

The vehicle models are designed in Simulink® and thereafter fed with input parameters and look-up-tables via Matlab®. This facilitates rapid simulations with an adjustment in examined variables. A not unimportant advantage in Simulink® is its graphical user interface, which facilitates an easy overview of the complex systems.

Other accessible programs are Modelica, Advisor, CRUISE, Vehicle Simulation Program (VSP) (Van Mierlo, 2000), SIMPLEV, EHVSP, Hy-Sim (Bolognesia et al., 2001) and THEPS (Hellgren, 2004) just to mention some.

The topmost level of the simulation model is shown in Figure 5.1. The implementation of the sub models (battery, ICE, electric machine etc) is described in Appendix B.
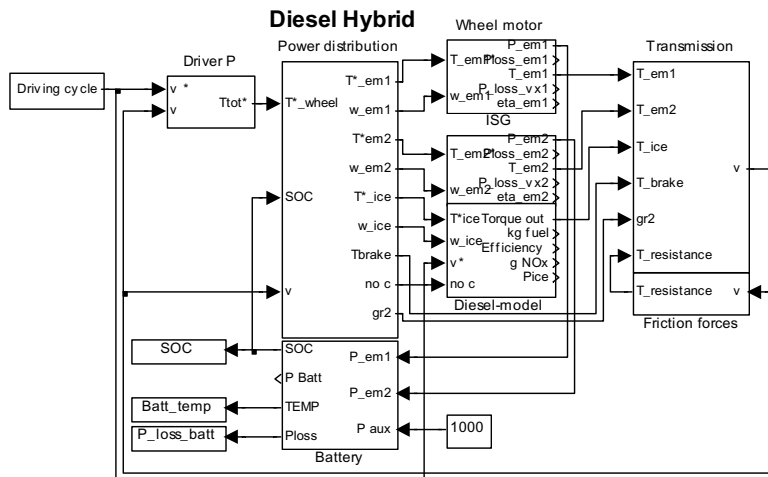
Figure 5.1:   The figure shows the topmost level in the simulation model. Each and
every modelled subsystem forms a separate block. In the simulation
model are submodels for driver, power distribution, electric machines,
ICE, transmission, friction forces and battery to be found as well as a
number of driving cycles.

5.1 Purpose of modelling

The aim with this study is to reduce fuel consumption and NO_X emissions
from a diesel electric parallel hybrid vehicle. For this purpose a simulation
model have been built, that describes all aspects of the vehicle that are
significant for the efficiency and NO_X formation estimation.

The intensions with the sub models are to model each component that
significantly affects fuel consumption and emissions separately. Separate
simulation blocks define the electric machines, ICE, battery, transmission
etc. All control algorithms, i.e. the onboard computers, are combined in one
block called power distribution. This mode of procedure facilitates the
study of the most important energy transformations in the HEV thoroughly.
The time scaling is chosen to facilitate a closer study in the matter of
transient behaviour of the ICE.

Key modelling parameters

Several parameters have a significant influence on performance, power consumption and emissions, such as chassis dynamics, efficiency of the electric machines and ICE and their maximum torque at different load points, battery state of charge (SOC) and temperature, driver behaviour. Last but not least the control of the power distribution between the sources of traction power has a significant influence.

The dynamic behaviour of the ICE is crucial when determining the emissions and the fuel consumption. Hence the time scaling is chosen to account for turbo lag and other dynamic effects in the ICE.

The simulation models are only simulating longitudinal movements of the vehicle, thus road slope, lateral and vertical forces are not taken into consideration.

The following part of this chapter will describe the equations of the simulation models. The vehicle sub models are presented in the following order;

- Chassis

- Electrical machines

- Power electronics

- Driver model

- Control system

- Engine models (petrol and diesel)

- Cylinder deactivation

- Gear shifting

At the end a verification of the model is presented. The implementation of the work itself, in Simulink, can be studied in detail in Appendix B.

When referring to electric machine 1 or 2 and gearbox 1 or 2 etc below, see Figure 2.1 and Figure 5.1.

Chassis dynamics

The sub model describing the chassis includes both the transmission and the friction forces acting on the vehicle. In the transmission sub model all longitudinal forces are added and the vehicle speed is obtained. Equation 5.1 describes the vehicle speed with forces expressed as wheel torques.

$$\frac{dv}{dt} = \frac{1}{r_{wheel}} \frac{1}{M_v} \left(T_{brake} + T_{\text{resistance}} + T_{em1}gr_1 + gr_1gr_2 \left(T_{ICE} + T_{em2} \right) \right) \qquad (5.1)$$

r_{wheel} = wheel radius, M_v = vehicle mass, T_{brake} = break torque, $T_{resistance}$ = resistance torque, T_{em1} = torque, electric machine 1, gr_1 = gear ratio, gearbox 1, gr_2 = gear ratio, gearbox 2, T_{ICE} = ICE torque and T_{em2} = torque, electric machine 2.

The vehicle friction forces can be described with the following relations. The friction force, i.e. the resistance torque $T_{resistance}$, is one of the inputs in Equation 5.1 above (Heywood, 1988) (Equation 5.2 - 5.3).

$$P_r = \left(C_r M_v g + \frac{1}{2} \rho_a C_d A_v S_v^2 \right) S_v \qquad (5.2)$$

$$T_{resistance} = \frac{P_r}{S_v} r_{wheel} \qquad (5.3)$$

P_r = resistance power, C_r = rolling resistance, M_v = vehicle mass, g = gravity, ρ_a = air density, C_d = air resistance, A_v = vehicle front area, S_v = vehicle speed

This is not the only way of describing the road load of a vehicle. Speed measurements on, and simulations of, a hybrid bus show that if a quadratic speed depending term is added, the modelling error decreases (Andersson, 2004a). The quadric dependence comes from the tires rolling resistance. Rolling resistance changes with speed. The measurements and simulations resulted in Equation 5.4.

$$P_r = \left(C_r M_v g + C_{r2} Mg S_v + \frac{1}{2} \rho_a C_d A_v S_v^2 \right) S_v \qquad (5.4)$$

P_r = resistance power, C_r = rolling resistance, C_{r2} = second rolling resistance term, M_v = vehicle mass, g = gravity, ρ_a = air density, C_d = air resistance, A_v = vehicle front area, S_v = vehicle speed

Equation 5.4 corresponds to the formula used by vehicle industry in connection with the vehicle hosting the original diesel engine, who's engine maps are used in the simulation model. See Equation 5.5.

$$P_r = \left(F_0 + F_1 S_v + F_2 S_v^2\right) S_v \qquad (5.5)$$

P_r = resistance power, F_0, F_1 and F_2 = road load and aerodynamic losses (given constants and not adjusted), S_v = vehicle speed

To stress the differences between Equation 5.2 and Equation 5.5 the simulation model has been adjusted to correspond to the vehicle that includes the original engine. Simulation results of resistance power when using Equation 5.2 and 5.5 respectively are shown in Figure 5.2. As can be seen in the figure Equation 5.4 consistently implies slightly larger resistance power. The difference decreases as the speed increases. This can be explained with the added term that is quadric speed dependent.
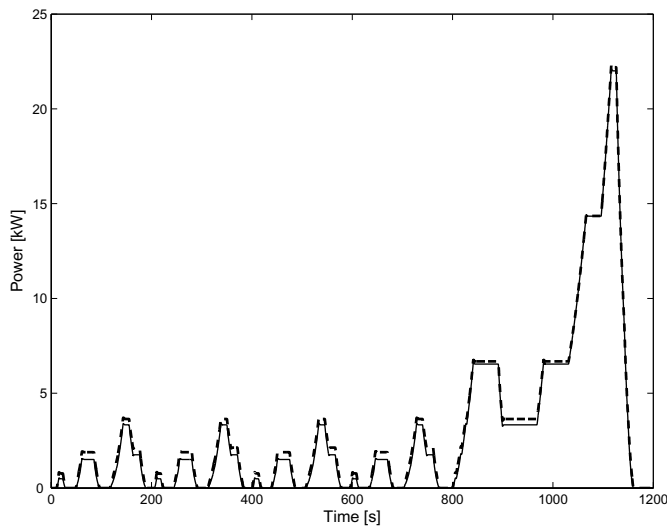
Figure 5.2:   The figure shows resistance power when using Equation 5.2 (dashed) and Equation 5.5 (solid) when running the simulation model in driving cycle ECE+EUDC.

Since both measurements show, and the vehicle industry apply the use of the quadric term, Equation 5.5 is used in the simulation model to describe the friction forces acting on the vehicle.

Electric machines and power electronics

The electric power drawn from the battery, from each electric machine in the simulation model, is obtained through Equation 5.6 (electric machine 1 is used as example). All machines are modelled in the same manner, but able to model with unique figures. The two modelled properties of the machines are the efficiency and the torque limitation. In Equation 5.7 the torque is limited to the maximum torque and in Equation 5.8 to maximal power.

$$
P_{em1} = \begin{cases} \dfrac{\omega \cdot T_{em1}^{*}}{\eta_{em1}} & when \quad \omega \cdot T_{em1}^{*} > 0 \\ \omega \cdot T_{em1}^{*} \cdot \eta_{em1} & when \quad \omega \cdot T_{em1}^{*} < 0 \end{cases}
\tag{5.6}
$$

$$
T_{em1}^{*} = \begin{cases} T^{'} & when \quad T^{'} < T_{max} \\ T_{max} & when \quad T^{'} > T_{max} \end{cases}
\tag{5.7}
$$

$$
T^{'} = \begin{cases} T_{em1}^{*} & when \quad T_{em1}^{*} \cdot \omega < P_{max} \\ \dfrac{P_{max}}{\omega} & when \quad T_{em1}^{*} \cdot \omega > P_{max} \end{cases}
\tag{5.8}
$$

The efficiency of the electric machine, η_{em1}, is dynamically adjusted with respect to speed and torque. Depending on the instantaneous torque and speed, a look-up-table will deliver the efficiency at the present load point.

The power electronic losses are represented in Figure 5.3 (upper) as a normalized efficiency table. In Figure 5.3 (lower) the normalized values for efficiency in an electric machine are shown.
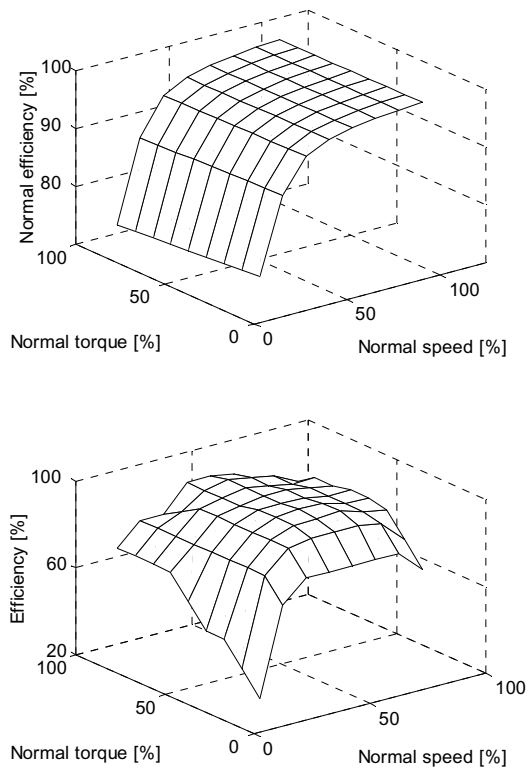
Figure 5.3:   The upper figure shows the normalized value for power electronic losses. The lower figure shows the normalized values for efficiency in an electric machine.

These two efficiency tables can as an approximation be multiplied into one, i.e. the efficiencies are multiplied with each other and a new table is obtained. This is possible since the speed is roughly proportional to the voltage and the torque is nearly proportional to the current. This table, representing efficiency in the electric machine including the power electric losses, is shown in Figure 5.4. This table is then used in the simulation model to represent the entire drive since it includes the influences from the power electronics.
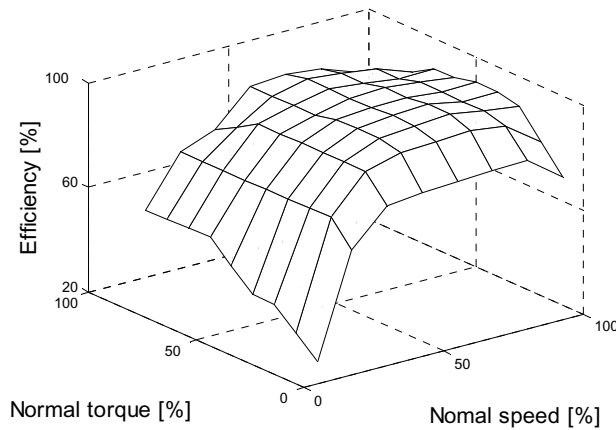
Figure 5.4:   The normalized value for efficiency in an electric machine, including the power electric losses.

The time constants describing the dynamics of the electric machines are much shorter than those describing the ICE or the chassis dynamics. Therefore the resolution in time in the simulation model is chosen with regards to the ICE, not the electric drives.

Battery

The battery model represents the battery losses that act on the battery power, ΔP. ΔP is the sum of all electric power that flows out of the battery. See Equation 5.9.

$$\Delta P = P_{em1} + P_{em2} + P_{aux} \tag{5.9}$$

P_{em1} = power to electric motor 1, P_{em2} = power to electric motor 2 and P_{aux} = power needed to auxiliary, that is air condition, fan etc.

The power used to charge or discharge the battery, P_{batt}, and the battery losses, P_{loss}, are calculated in the following way (Equation 5.10 and Equation 5.11), when ΔP is positive, i.e. the battery is discharged:

$$P_{loss} = \left| \Delta P - \Delta P \eta_{batt} \right| \tag{5.10}$$

$$P_{batt} = \Delta P \eta_{batt} \tag{5.11}$$

η_{batt} is the battery efficiency and $\eta_{batt} < 1$ when $\Delta P < 0$ and $\eta_{batt} > 1$ when $\Delta P > 0$ (see Figure 5.6).

The battery efficiency, η_{batt}, is dynamically adjusted depending on the present SOC, battery thermal power ΔP. The total battery efficiency consist actually of two separate parts, one depending on the prevailing SOC and one depending on the battery power electronics (*PE*), see Equation 5.12.

$$\eta_{batt} = \eta_{batt(SOC)} \cdot \eta_{batt(PE)} \tag{5.12}$$

In the simulation model, the battery is modelled as a resistance model (see Figure 5.5). The fundamental battery equations are shown in Equation 5.13 - 5.17 (Alaküla, 2004).
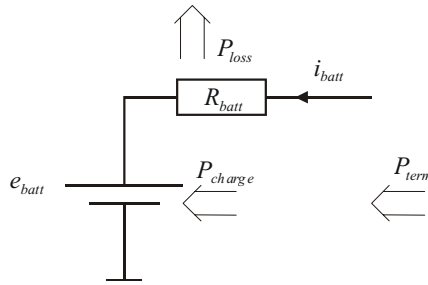
Figure 5.5: The figure shows a schematic model of the battery model, used in the simulation model.

$$P_{term} = (e_{batt} + R_{batt} \cdot i_{batt}) \cdot i_{batt} = e_{batt} \cdot i_{batt} + R_{batt} \cdot i_{batt}^2 \tag{5.13}$$

$$i_{batt} = -\frac{e_{batt}}{2 \cdot R_{batt}} \pm \sqrt{\left(\frac{e_{batt}}{2 \cdot R_{batt}}\right)^2 + \frac{P_{term}}{R_{batt}}} \tag{5.14}$$

$$P_{loss} = R_{batt} \cdot i_{batt}^2 \tag{5.15}$$

$$P_{charge} = P_{term} - P_{loss} \tag{5.16}$$

$$\eta_{batt} = \frac{P_{charge}}{P_{term}} \tag{5.17}$$

In 5.13 - 5.17 P_{term} is terminal power, $e_{batt} = f(SOC)$ and is battery voltage, $R_{batt} = f(SOC)$ and is battery resistance, i_{batt} is battery current and P_{charge} is charging power.

The battery model is based on physical data originating from the Toyota Prius 1st generation (Toyota Motor Corporation, 2000), when such have been available. Supplementary data have been used from battery measurements (Johnson et al., 2001). These data are mould together into a look-up-table with ΔP and SOC as inputs and the battery efficiency, $\eta_{batt(SOC)}$, depending on SOC as the output. See Figure 5.6.
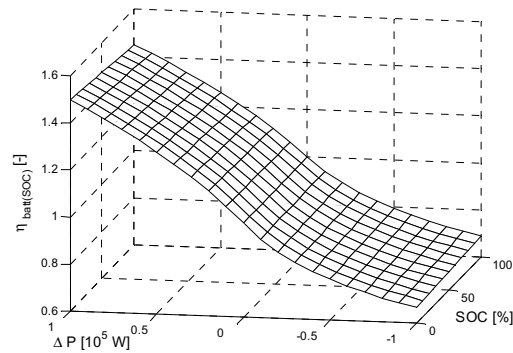
Figure 5.6: Battery efficiency as function of ΔP and SOC. The scale on the x-axis can be regarded as relative power supply. When the efficiency >1 the battery is charging and because of the losses the power supply to the battery must be >1 if the battery should be able to fully charged. When the efficiency is <1, the battery is discharging. That is that there are losses causing the efficiency of the supplied battery power to be <1.

The influence of the power electronics in the battery has been modelled as a normalized efficiency table, see Figure 5.7.
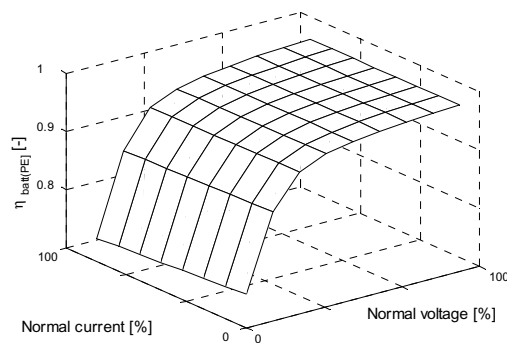
Figure 5.7: The normalized value for power converter efficiency.

Figure 5.6 and Figure 5.7 represent together η_{batt} in Equation 5.10 and 5.11.

The SOC of the battery is calculated as an integral of the power, reduced by the battery losses according to Equations 5.18 and 5.19. P_{loss} is depending on whether ΔP is positive or negative, i.e. if the battery is charging or discharging.

When the battery is charging:

$$SOC = \frac{1}{W_{batt,max}} \int (P_{batt} - P_{loss}) dt \qquad (5.18)$$

When the battery is discharging:

$$SOC = \frac{1}{W_{batt,max}} \int (P_{batt} + P_{loss}) dt \qquad (5.19)$$

A thermal model is included with one thermal node inside the battery pack for a rough estimate of the battery temperature with the various control methods. The battery temperature arises from the assumptions and premises described below.

The thermal equilibrium in a homogeneous body can be expressed by Equation 5.20.

$$\frac{dT_{emp}}{dt} = \frac{(P_{loss} - P_{cool})}{C_{batt\_thermal}} \qquad (5.20)$$

$\quad C$ = thermal capacity

The cooling losses in a homogeneous body can be described in the manner shown in Equation 5.21.

$$P_{cool} = \frac{T_{emp} - T_{outer}}{R_{batt\_thermal}} \qquad (5.21)$$

That gives the expression in Equation 5.22.

$$\frac{dT_{emp}}{dt} = \left(\frac{1}{C_{batt\_thermal}} \left(P_{loss} - \left(\frac{(T_{emp} - T_{outer})}{R_{batt\_thermal}} \right) \right) \right) \qquad (5.22)$$

This simple battery temperature model is present in the simulation model, but not used in the analysis made in this thesis.

Driver model

The driver is designed as a simple *PI*-controller with anti-windup on the integrator to prevent saturation in the actuator (Årzén, 2000). The necessary amount of wheel torque to achieve the requested vehicle speed is calculated with Equation 5.23 and 5.24. The requested speed is given by drive cycles as look-up-tables.

$$F_{tot}^* = K\left(\left(v^* - v\right) + \frac{1}{s\tau_i}\left(v^* - v\right) \right) + \frac{1}{\tau_t}\left(u - v_{controller}\right) \tag{5.23}$$

F_{tot}^* = total requested force, $v_{controller}$ = output of the controller, u = actuator output

$$T_{tot}^* = F_{tot}^* r_{wheel} \tag{5.24}$$

T_{tot}^* = total requested torque, r_{wheel} = wheel radius

With no saturation the expression (u-$v_{controller}$) approaches zero, i.e. no windup and hence no use for the tracking time constant, τ_t.

The tracking time constant is supposed to be larger than τ_d and smaller than τ_i. In the model it has been sized by the rule of thumb that is shown in Equation 5.25.

$$\tau_t = \sqrt{\tau_i \tau_d} \tag{5.25}$$

It is important to keep in mind that the model is a rough and conscious simplification of the behaviour of a driver. This simplified driver is suitable for comparative studies, though less accurate for absolute studies of specific driver behaviour.

Power distribution

The considerations that controls the power flows are taken in the sub model called the power distribution block. This block represents the computer power onboard the vehicle. It calculates the references for the required torque from each of the main energy converters. These torques are calculated as a function of the instantaneous tractive power demand, the

auxiliary power demand, the deviation of SOC in the battery and finally the actual speed of the vehicle and the different machines.

A fundamental consideration within this block is that the dynamic operation of the ICE must be limited. The simplest way to limit the dynamic operation of the ICE is to low pass filter the ICE power requirement. See Figure 5.8. The time constant of the filter must thus be selected to ensure quasi-stationary operation of the ICE. The ICE power requirement is thus given by Equation 5.26.
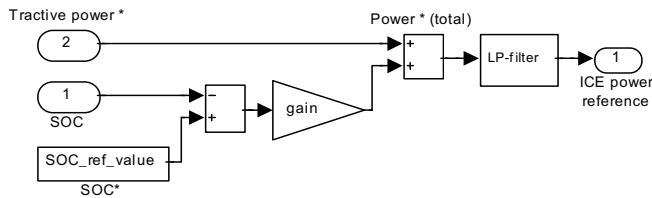
Figure 5.8:   A generalized view of the part of the power distribution block in the simulation models that handles the calculation of ICE power reference.

$$\frac{dP_{ice}^*}{dt} = \frac{P_{tractive} + P_{aux} + k(SOC^* - SOC) - P_{ice}^*}{\tau_{ice}} \qquad (5.26)$$

The stationary efficiency or emissions of an ICE can be expressed in a map as a function of speed and torque. This disregards dependence of temperature and ageing etc. From this map the best operating point for any power level within the ICE's operating range can be selected. Figure 5.9, the upper part, shows the efficiency map and the lower part shows the optimum torque and efficiency as a function of the requested power derived from the efficiency map for a diesel engine.
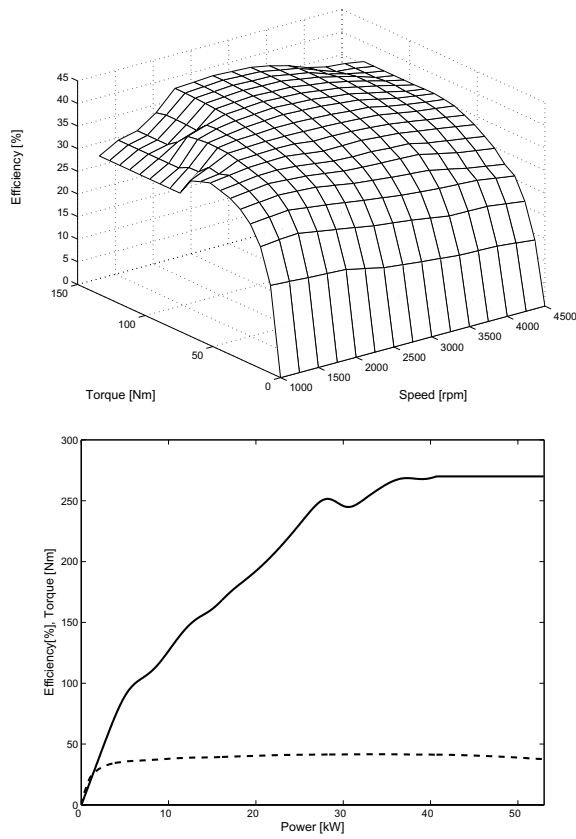
Figure 5.9:   Upper: Efficiency map for diesel engine. Lower: Available torque when
               running the diesel engine at optimal load point (solid line). ICE
               efficiency at optimal load point for a diesel engine (dashed line).

The torque and speed references for the ICE are calculated from the
demanded power, $P_{ice}*$, via a look up table like the one in Figure 5.9, the
lower, in the hybrid model. The references are being denoted $T_{ice}*$ and
$\omega_{ice}*$. The ways to realize these references are slightly different for the
different hybrids. Equations 5.27 and 5.28 display how the reference torque
and speed are selected.

$$T_{ice}^* = f(\omega_{ice}, \tau_{ice}) = "look-up-table" \text{ (See Figure 5.9)} \tag{5.27}$$

$$\omega_{ice}^* = \frac{P_{ice}^*}{T_{ice}^*} \tag{5.28}$$

To increase the efficiency of the ICE, it is controlled to only operate at efficiencies above a predetermined limit. The limit is controlled with hysteresis, to avoid a "nervous" switching on and off of the ICE. The ICE torque demand is then switched on at η_{ICE} = 23% and switched off at η_{ICE} = 22% for the petrol engine and 30% and 34% respectively for the diesel engine. The higher efficiency levels for the diesel engine is due to its higher total efficiency. These efficiency limits originates from a comparison of possible power flows.

The power that causes the wheel torque originates from the fuel since there is no possibility to charge the vehicle from the grid. The power has two paths to choose from: from well to wheel via ICE or via ICE, electric machines, battery and power electronics. The latter path includes increased losses compared to only use the ICE. This implies a maximal efficiency for the hybrid path (ICE, electric machines etc) below the conventional path (only ICE). The hysteresis limits are based on the assumption that the average efficiency of the electric machines is 92%, the power electronic converter is 96%, and the battery charge/discharge efficiency is 90%. Assuming that the energy that leaves the battery for traction originates from the ICE at peak efficiency (40%), then the "brake even" efficiency of the ICE is $0.4*0.92^2*0.96^2*0.9=0.28$, i.e. if the ICE efficiency is higher than 28%, then it is better to let the energy flow from the ICE, otherwise the ICE should be turned off. In the simulation program, this window is set somewhat higher.

Switching the ICE on and off at fixed efficiency limits as is done in this context is certainly a simplification. It would have been better to make these limits dynamic and functions of the present, and past, operating points. The development of a strategy to accurately set such dynamic limits is however a big task in itself and beyond the scope of this thesis work.

Parallel hybrid strategy

Since the ICE in the parallel hybrid is mechanically connected to the wheels (see Figure 2.1), the speed reference for the ICE can only be reached if the gearbox is able to set up a suitable gear ratio (gr_2) given the instantaneous combination of vehicle speed and ICE speed reference. The most suitable gear ratio is selected and a set of new references for the ICE torque and speed are calculated by Equations 5.29 and 5.30.

$$gr_{2,min} < gr_2 = "\frac{v_{vehicle}}{r_{wheel} \cdot \omega_{ice}^* \cdot gr_1}" \text{ in 6 fixed steps} < gr_{2,max} \tag{5.29}$$

$$\omega_{ice}^{*'} = \frac{\dfrac{v_{vehicle}}{r_{wheel}}}{gr_1 \cdot gr_2} \quad \text{and} \quad T_{ice}^{*'} = \frac{T_{ice}^* \cdot \omega_{ice}^*}{\omega_{ice}^{*'}} \tag{5.30}$$

Given the new set of ICE torque and speed references, the torque references for the electrical machine(s) are calculated according to Equation 5.31 and 5.32. Since the simulation model contains two electric machines, the torque demand is distributed proportional to the best of their ability given the operating conditions. Consideration is taking to the two gearboxes included in the model.

$$T_{em1}^* = \frac{T_{wheel}^* - \left(T_{ice}^* \cdot gr_1 \cdot gr_2\right)}{gr_1} \cdot \frac{T_{em1,max} \cdot gr_1}{T_{em1,max} \cdot gr_1 + T_{em2,max} \cdot gr_1 \cdot gr_2} \tag{5.31}$$

$$T_{em2}^* = \frac{T_{wheel}^* - \left(T_{ice}^* \cdot gr_1 \cdot gr_2\right)}{gr_1 \cdot gr_2} \cdot \frac{T_{em2,max} \cdot gr_1 \cdot gr_2}{T_{em1,max} \cdot gr_1 + T_{em2,max} \cdot gr_1 \cdot gr_2} \tag{5.32}$$

If only one machine is used, the specification for the other of the two in the model is set to zero maximum torque in Equation 5.31 and 5.32. The maximum torque values, used in Equation 5.31 and 5.32, are momentary values taking field weakening into account, and do thus vary continuously with speed.

5.2 Engine models

HEVs facilitate using the ICE only at high efficiency since the presence of electric machine(s) make it possible to switch off the ICE at low efficiencies and thus use pure electric traction.

One intension with the simulation model is to take advantage of the higher efficiency of the diesel engine compared to the petrol. The maximum efficiency of a petrol and diesel engine respectively are shown in Figure 2.5.

Petrol

As earlier mentioned the ICE petrol sub model is made by Petter Strandh at Combustion Engines, Department of Heat and Power Engineering, Lund University, as a part of his licentiate thesis (Strandh, 2002). A detailed description of the ICE model is available in his thesis. Here follows a brief description of the ICE model.

The ICE model describes a naturally aspirated gasoline engine. Input data consist of engine speed and torque demand. Outputs are composed by actual torque, fuel consumption and emissions (HC, NO_X and CO).

The model tries to deliver the demanded torque as accurately as possible while taking the different dynamic phenomena in the inlet manifold and fuel flow characteristics into consideration. A simplified description of the inlet manifold is a low pass filter with a time constant of about 0.1s.

The fuel calculations include equations that describe the wall-wetting model. That is how much of the injected fuel that instantaneously enters the engine and how much of the injected fuel that is stuck to the walls of the inlet port.

There is also a closed loop model for adjusting the fuel injection to achieve the desired stoichiometric air/fuel mixture ($\lambda = 1$).

To form the engine torque the airflow and engine speed are needed. The engine speed is known and the airflow is derived from the manifold and throttle sub model. By using these two variables as input in a look up table, the torque at stoichiometric conditions is derived. This torque is thereafter corrected to achieve the torque at the current λ-value.

An interesting parameter in a study like this is the engine size. The size is depending on dominating load point of the application and engine efficiency. The maximum efficiency for a naturally aspirated SI engine can be found at full torque and about the middle of the engines operating speed range. So in order to minimize the fuel consumption, the engine size should be chosen in such way that the dominating load points of the application, in this case the hybrid vehicle, are found within this region.

The scaling of the ICE has been achieved by changing the number of cylinders. By this procedure it is reasonable to assume that the engine maintains its main characteristics, apart from the torque.

A real engine has been tested in transient operation and data has been logged. Afterwards the model engine has been run according to the same driving cycle. These measured and calculated data for air fuel ratio are shown in Figure 5.10. The upper curve shows how the air fuel ratio differs between the real engine and the simulated engine. The lower curve is the torque change. Conclusions from the graph is that the wall-wetting model, to some extent describes the wall wetting that occurs in the real engine. (Strandh, 2002)
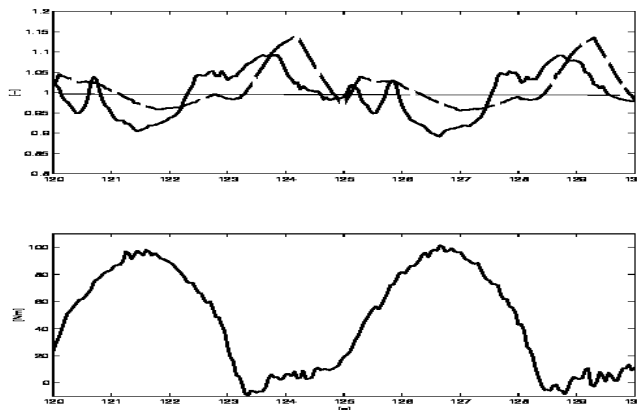
Figure 5.10:   Upper graph: Dashed line is the simulated air fuel ratio and the solid line is taken from real engine tests. Lower graph: torque changes, real data.

The way that the model has been built makes it possible to simulate other naturally aspirated makes and sizes of engines. This is achieved by modification of the air map, the inlet manifold size and the exhaust manifold size combined with control parameters from the engine control unit.

In the present model, emissions are calculated using values that have been measured after the catalyst. When the engine operates in a transient mode, during a fast load change and when the fuel/air ratio is deviated from $\lambda=1$, the emissions are assumed to increase by the same percentage as the emissions increase before the catalyst. Thus, it is assumed that the conversion efficiency of the catalyst is maintained outside the λ-window. This could be the case for fast and not so large lambda deviation, due to the storage capability of the catalyst.

Diesel

The diesel engine modelled describes a state of the art diesel engine in 2004. The engine data is scaled to fit the size of the vehicle used in the case study. The originally engine is approximately twice the size of the engine in the reference vehicle. The scaling is accomplished by reducing the piston displacement by decreasing the piston diameter. This involve increased friction surface, i.e. most likely slightly decreased ICE efficiency. These losses are not taken into consideration in the simulation model. The objectives are rather to study the relative effects of the control strategies and the chosen method allows this.

Input data are the demanded torque and vehicle speed, actual engine speed and the number of cylinders when simulating the model with cylinder deactivation. Outputs are the actual engine torque, fuel consumption, NO_X and when applicable the urea consumption. Fuel consumption and NO_X are determined by using look-up-tables formed by measured data. The engine temperature, needed to determine the conversion of NO_X thanks to SCR, is also received from a look-up-table.

The model includes no transient correction when rapid workload changes are undertaken. The time constant in the charging strategy in the hybrid vehicle results in slower transients in demanded power than in the conventional vehicle. Since the simulation shows accuracy in comparison with measured values (see Table 4), the assumption is considered as sufficiently accurate.

5.3 Cylinder deactivation

Driving a conventional vehicle in city traffic is usually not efficient. This is due to the low power demand relative to the large amount of power available. This implies that the efficiency rarely reaches the higher levels in city driving. A smaller engine, adapted for city traffic would increase the efficiency, but would also imply inability to drive in highway traffic due to an unreachable power demand. The advantage with a hybrid vehicle run in city traffic is the possibility to run in electric mode at low power demands and use the ICE at larger power demands or use combinations of thereof.

The optimum, regarding efficiency, should be to be able to switch between a larger and a smaller engine depending on the power demand. This is however possible to achieve by means of cylinder deactivation.

As described, in Chapter 4.2, deactivating cylinders involve losses. These losses increases with engine speed, see Equation 5.33. The losses are added in the simulation model to the total power demand when running the engine in deactivated mode.

$$P_{loss} = T(\omega)_{loss, deactivated\ engine} \cdot \omega \qquad (5.33)$$

The look-up-tables used to describe the engine model are there after scaled to correspond to the new size of the deactivated engine, i.e. in this example maximum torque and maximum power is multiplied with a factor 0.5.

5.4 Gearshift control

The choice of gear ratios affects the hybrid vehicle performance significantly. The simulation model has been provided with a number of different gearboxes, besides the one belonging to the used motor data. Both gear ratio and final gear ratio have been adjusted.

The gearbox belonging to the reference vehicle on which the measurements have been carried out have initially been used in the simulation model. It is shifted as a function of speed. Gear shifting as function of speed is a standard method for evaluating fuel consumption in a conventional vehicle, where the ICE is the only power supply. In a hybrid vehicle the speed of the ICE is not depending on the vehicle speed to the same extent. To obtain an advantage of the hybridisation the gear shifting is changed from being speed related to follow the best gear ratio according to the present ICE speed and ICE torque demand.

Since the hybrid vehicle can be supplied with power from the electric machine, besides the ICE, other strategies have been examined. Such strategies are shift due to best possible instantaneous gear ratio, due to lowest fuel consumption of lowest NO_X. Adjusting the gear steps (equidistant and logarithmic) and/or the final-drive ratio has also been implemented. Simulations with more gears than usual have been carried out as well.

The ICE is not needed for tractive power supply at low speeds when running a hybrid vehicle assuming that the electric power available is enough. Therefore the gear ratio for gear 1 has been decreased. The gear ratios for the gears 2…(n-1) have also been adjusted. This means that it is easier to control the engine to operate close to the optimal load point. The

idea is based on a study of the maximum wheel torque at the first gear, considering the original gear ratio. This study is carried through for the original engine as well as for the hybrid vehicle (ICE and electric machines together). This results in a slightly higher available wheel torque for the hybrid vehicle, +/-3.3% to be exact. The gear ratio for the hybrid vehicle is then reduced to make the maximum available wheel torque of the hybrid equal to the corresponding torque of the conventional vehicle. This has been carried out in the manner of reducing the gear ratio for the lowest gear. The gear ratio for the highest gear has been retained. The difference between highest and lowest gear ratio has been distributed as shown in Equation 5.34 where n is number of gears.

$$\text{gear ratio}_{1...n} = \text{gear ratio}_1 * k^{0...(n-1)}$$
$$k = \sqrt[(n-1)]{\frac{\text{gear ratio}_n}{\text{gear ratio}_1}} \tag{5.34}$$

5.5 Verification

The measured data belonging to the diesel engine in question includes also test results from drive cycle test in a vehicle available on the market. The ECE+EUCD test cycle has been used in these test, see Figure 5.11. The cycle can be divided into two parts 0 - 780 s. and 780 - 1180 s. The first part (ECE) is considered as the urban cycle and the last part is considered the extra-urban part (EUCD).
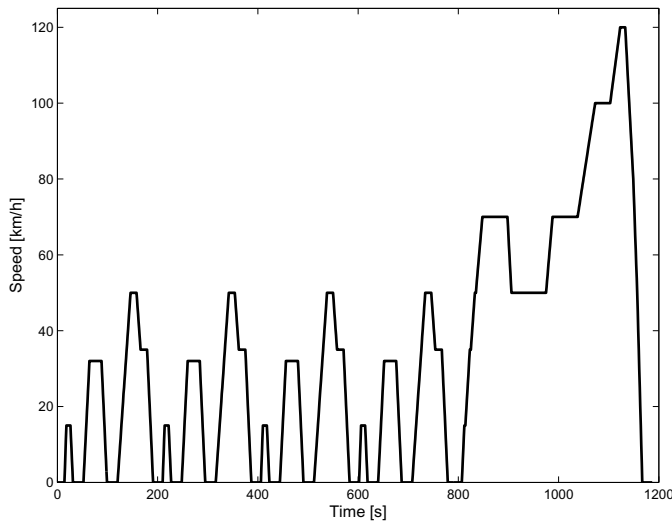
Figure 5.11:   Test cycle ECE+EUCD.

To verify the simulation model, the target vehicle has been adjusted to be equivalent to the actual test vehicle regarding vehicle mass, roll- and air resistance, engine power, wheel radius and maximum vehicle speed. The result of the simulations can be seen in Table 4.

Table 4: Verification results, fuel consumption [l/100 km].

	Urban (0 – 800 s):	**Extra-urban** (800-1200 s):	**Combined** (0-1200 s):
Test results	7.7	4.9	5.9
Simulation	8.1	5.4	6.2

The results do not fully correspond to the measurements. The measurements that constitute input value in the simulation model do not reach to idle speed, that is 850 rpm. The look-up-table ends at 1000 rpm. That implies that idle speed will be higher in the simulation than in reality. Hereby the fuel consumption will increase as well.

Other possible issues that accounts for the differences in fuel consumptions are, for example, uncertainty in choice of road load function in the test results. Neither is there any information available if measured vehicle data origin from exactly the same engine that the data in the look-up-tables derive from. The engagement of the attachments might also be overestimated in the simulation model. Finally there are differences in

driving a vehicle in reality, which includes transients, in comparison with quasi-stationary calculations carried out in the simulations. This is not accounted for. These reasons might form the underlying causes that combine to the differences shown in Table 4.

As far as NO_X is concerned, the emissions for the simulated vehicle amount to 0.47 g NO_X/km. The engine data is adapted to the Euro 3 levels, that is 0.50 g NO_X/km. That means that the simulation model manages the emissions regulations despite increased fuel consumption compared to the measured data.

Chapter 6

Case study

The model described in the previous chapter has been used for a case study. The simulated vehicle has been implemented as equal a Toyota Prius generation 1, as possible. The engine has however been replaced with a diesel engine.

6.1 Driving cycles

The simulations have been carried out with the test cycle ECE+EUDC, see (Figure 6.1 and Figure 6.2). The driving cycle is also known as MVEG-A-cycle and is used for emission certification of light duty vehicles in Europe. The cycle consists of four ECE segments (0-780 s in Figure 6.1), which are repeated without interruption. This is then followed by one EUDC segment (780-1180 s in Figure 6.2).
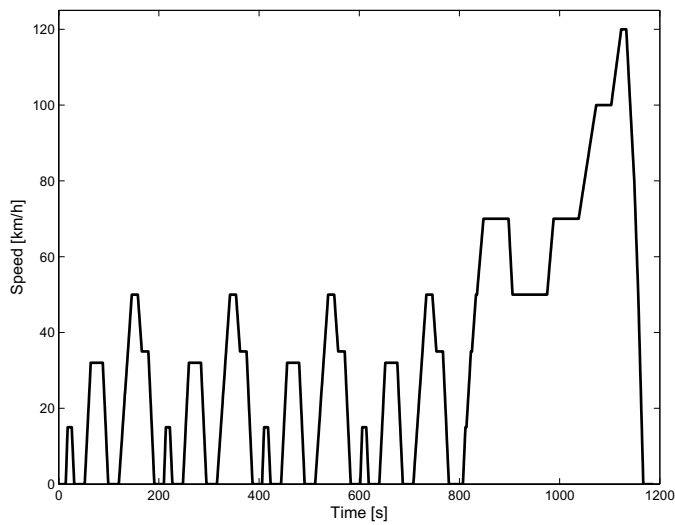
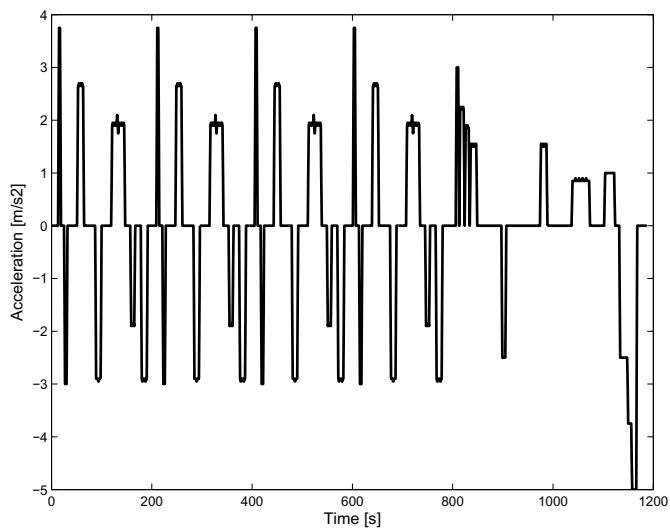Figure 6.1:   Drive cycle ECE+EUDC, velocity.

Figure 6.2:   Drive cycle ECE+EUDC, acceleration.

The ECE cycle represents an Urban Driving Cycle and is therefore also known as UDC. It is characterized by low vehicle speed and low accelerations, which for a normal passenger car gives low engine load and low exhaust gas temperature.

The last segment, EUDC (Extra Urban Drive Cycle), is added to account for more aggressive, high speed driving modes. It contains a maximum speed of 120 km/h. There is an alternative EUDC cycle intended for low powered vehicles. Its maximum speed is 90 km/h.

The total distance of the driving cycle is 11 km and the maximum speeds are 50 km/h in ECE and 120 km/h in EUDC respectively. The average speed is 33.4 m/s and the maximum acceleration is 3.75 m/s^2. (Dieselnet, 2005a)

6.2 Reference vehicle

To make the survey fair and relevant to a large market segment, a medium sized family car has been chosen as simulation input. The specific vehicle is Toyota Prius, an electric hybrid family car, available on the market today. The advantages with the choice are that input data are accessible and there are measured data available as well.

The chosen Toyota Prius is the one marketed in Europe 2002 (Jonasson, 2002). A newer model of Prius has reached the market since then, but that model has not been used in this survey. Further details about the model in question can be found in Appendix B.

As input in the ICE-simulation model for the petrol engine, data from a SAAB engine has been used. This is due to lack of sufficient detailed information about the Toyota Prius engine. The diesel engine model is based on data deriving from a state of the art diesel engine available on the market. This is due to that there is no diesel engine in the Toyota Prius.

The SAAB engine is a naturally aspirated gasoline engine, 2.3 l and 16 valves. Its max torque is 212 Nm at 3800 rpm and its max power is 110 kW at 5500 rpm. The engine data used in the model are all measured at Lund University, department of Heat and Power Engineering, Combustion Engines division.

The SAAB engine data is thereafter adjusted through scaling to suite the size of the Prius ICE (PRIUS, 2000). Input data in the simulation model are the engine speed and the torque demand. Outputs are the actual torque, the fuel consumption and the emissions. The emission output is derived from scaled emission maps, as based on the SAAB engine measurements.

The diesel engine is also scaled to correspond to the power of the Prius engine. The data originate from measurements performed by the manufacturer. The inputs and outputs variables in the diesel model are equal to the variables used in the petrol engine model.

The sizes of the electric machines are selected to correspond to the Prius data, as well as possible and adjusted to suit the demands following the topology. (See Table 5.) Note that the Prius is equipped with a power split hybrid topology.

Table 5: Vehicle data in simulation model.

Property:	Unit:	Prius:	Parallel:
$P_{max\ em1}$	kW	33	33
$T_{max\ em1}$	Nm	350	353
$\omega_{max\ em1}$	Rad/s	585	187
fwf [6]	-	5.4	2.0
$P_{max\ em2}$	kW	33	33
$T_{max\ em2}$	Nm	68	140
$\omega_{max\ em2}$	Rad/s	471	471
fwf	-	1.0	2.0
$P_{max\ ICE}$	kW	53	53
$T_{max\ ICE}$	Nm	115	134

6.3 Parameters

The hybrid application allows relatively independent control of engine load points. Therefore a consideration concerning load points is crucial. Load points representing the lowest fuel consumption does not coincide with those resulting in the lowest NO_X, rather the opposite. (Johnson et al., 2000) This can be seen in Figure 4.4. It is therefore of interest to investigate the influences when *controlling the ICE* to operate for lowest fuel consumption and thereafter for lowest NO_X.

The quantity of EGR affects the NO_X formation. Therefore an alternative *EGR strategy* is investigated as well as the one that originates from the engine data.

---

[6] fwf = field weakening factor

Another parameter that is studied is *SCR*, since it facilitates additional NO_X reduction. Simulations are performed with and without SCR.

Since the choice of gear ratios of the gearbox and final *gear ratio* also influences the feasible load points, its influences will be investigated too.

Deactivating a number of cylinders facilitates possibilities to utilize increased efficiency of the ICE. On account of this possibility, simulations *deactivating cylinders* are carried out as well.

To make the results comparable to as high extent as possible, the deviation in SOC at start and at stop is accounted for. This means that the fuel consumption is adjusted so the SOC ends at the same level as it started at. In a strict point of view this gives to a slightly incorrect level of emissions. The emissions are therefore adjusted with the same percent as the fuel consumption is adjusted with.

The investigated parameters are shown in Table 6.

Table 6: Investigated simulation parameters.

Parameters:	Alternatives:
Control strategy	Efficiency / NO_X
EGR	Original / increased
SCR	On / off
Gear box and final gear ratio	Original / altered
Deactivating cylinders	On / off

6.4 Previous results from petrol engine

In previous study (Jonasson, 2002) simulations where carried out on a model as equal as possible to a Toyota Prius. The simulation model included a petrol engine, exactly as the Prius does.

The simulations where compared with results from a research and test company in Sweden, called MTC AB. As a conclusion of the performed investigation of the Prius, the fuel consumption ended in the range 4.8 – 6.9 l/100 km when using the cycle ECE 15 (Karlsson, 2000). The driving cycle ECE 15 does not include the top speed of 120 km/h as the ECE+EUDC cycle does, see Figure 6.3, hence the results is not quite comparable with the results simulated in this study.
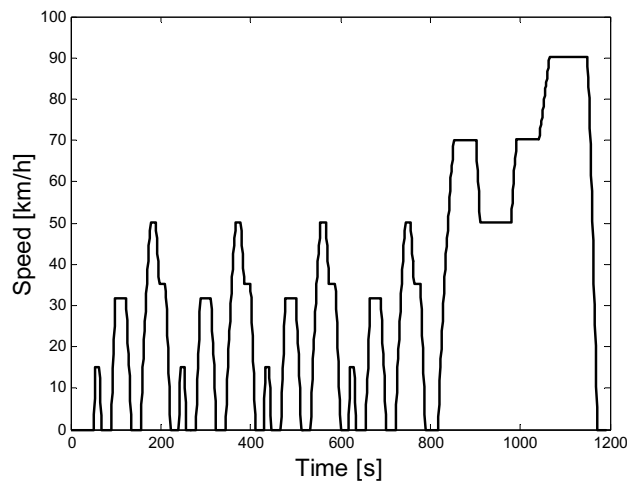
Figure 6.3:   Drive cycle ECE 15, velocity.

The result from the simulation of a petrol version of the Toyota Prius (Toyota Motor Corporation (2000), is shown in Table 7. The chosen results are those of a parallel electric hybrid vehicle. The table shows results when driving the cycle ECE+EUDC.

Table 7: Fuel consumption [l/100 km] and NO_X [g/km] when simulating a model of a parallel electric hybrid using a petrol engine in the driving cycle ECE+EUDC. Note that Euro 4 regulates NO_X for petrol cars to 0.08 g/km.

Fuel consumption (petrol):	NO_X:
5.8	0.24

The simulations results in higher emissions than what the survey carried out by MTC showed (Karlsson, 2000). This might indicate that there is adjustment to perform in the model of the petrol engine. It is therefore of interest to investigate if the lambda sensor could be speeded up. Additional actions to reduce the emissions could be to implement EGR or utilize NO_X storage. However, all these actions are beyond the focus of this study.

6.5 Results

In the simulations, carried out in this comparison and presented below, no other parameters are adjusted than those explicitly mentioned. Furthermore only one parameter at a time is varied, if not otherwise is stated. This is done since there are several parameters available in the simulation models. To simulate all those parameters, in all different combinations, would result in hundreds of simulations. Such a result flow would be impenetrable. If only two instances per parameters are investigated (more is possible for some of the parameters), it is nevertheless $2^7 = 128$ possible cases to compare. This figure does not include changes in the ICE, battery, electric machines, driving cycles etc.

This chapter presents a limited number of the results, in a selection of parameters, which are varied. The presented results are chosen to illustrate the impact the individual parameter has. The influences of the charging time constant and charging gain was investigated earlier (Jonasson, 2002).

Neither are the results from the petrol engine presented. The petrol engine is closely investigated in the previous study (Jonasson, 2002). The results presented below originate consequently from the diesel electric hybrid simulation model.

Control strategy

The means of control that are investigated are described in Chapter 4.2. As mentioned one of the advantages with hybrid vehicles is the possibility to relatively freely choose the ICE load points. In Table 8 the fuel consumption and NO_X emission are shown when choosing to optimize for NO_X emissions or ICE efficiency respectively. As comparison the consumption for a conventional diesel driven vehicle, equal in size etc, is shown. Table 8 should not be mistaken for the results shown in Table 4, which shows the measurements made up on the test vehicle.

Table 8: Fuel consumption [l/100 km] and NO_X [g/km] when controlling for minimal fuel consumption, controlling for minimal NO_X emission or for a conventional vehicle as equal an Toyota Prius as possible.

Optimization method:	Fuel consumption:	NO_X:
Efficiency:	4.4	1.33
NO_X:	4.9	0.69
Conventional:	5.6	1.03

The presented results originate from a conventional vehicle, with the same size as a Toyota Prius, and with a diesel engine. This implies that the engine model is scaled compared to the original engine. In this simulation the engine is forced to use load point where the impact of emission control is reduced. This is the reason why the engine does not manage the emission regulations in Table 8.

It is expected that the emissions decrease when running a control algorithm with the main purpose to minimize the emission. Running a hybrid implies that other load points are used than in a conventional vehicle. The ICE efficiency optimized hybrid vehicle aims to operate at high engine efficiency. The chosen load point that includes high efficiency, coincides to some extent with the maximum value for NO_X emissions, see Figure 4.4. When running an engine made for conventional vehicles as a hybrid, this is one of the results. One of the conclusions hereof is therefore that the emissions must be controlled for the hybrid application.

When optimizing for high diesel engine efficiency the fuel consumption decreases. The fuel consumption for the control strategy optimizing for NO_X results in slightly greater fuel consumption, since the load points including low NO_X implies lower ICE efficiency. These results were in other words expected. The optimal choice of load points when running for highest ICE efficiency is shown in Figure 6.4 as well as the outcome of the simulation. Figure 6.7 shows corresponding results when optimizing for NO_X emission.

Figure 6.6 and Figure 6.9 show operating diagrams. The z-axis shows the frequency of how often the load points are used.

There is also a difference in optimizing for high ICE efficiency and optimizing for low fuel consumption. Optimizing for high engine efficiency implies that the engine is switched off under a certain efficiency level. That

implies in its turn that the battery supplies with power at these occasions and there are losses in the battery, electric machine, power electronics etc. These power losses are consumed fuel that becomes heat instead of kinetic energy. This might lead to a low overall efficiency for the vehicle despite the high engine efficiency. A better strategy for switching the ICE on and off would account for system efficiency and the battery charge history in a way that is beyond the scope of this thesis to include. Such a strategy is however only expected to improve the fuel consumption a little, if any, compared to the strategy used here.

Figure 6.4: The figure shows the *efficiency map* and results from simulation with optimal ICE efficiency as control strategy. The optimal choice of load points considering ICE efficiency is indicated as a solid black line. The chosen load points when driving ECE+EUDC are shown as red dots.
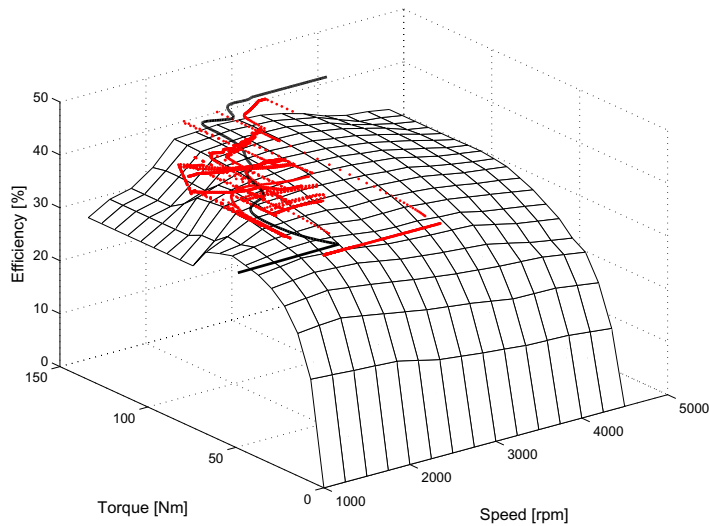
Figure 6.5:   The figure shows the *NO_X emission map* and results from simulation with
                optimal ICE efficiency as control strategy. The optimal choice of load
                points considering lowest NO_X is indicated as a solid black line. The
                chosen load points when driving ECE+EUDC are shown as red dots.

Figure 6.6: The figure shows an operating diagram when simulating the driving ECE+EUDC with optimal ICE efficiency as control strategy. The z-axis shows the frequency of how often the load points are used. Note that the main focus coincide with the optimum line (see Figure 6.4).
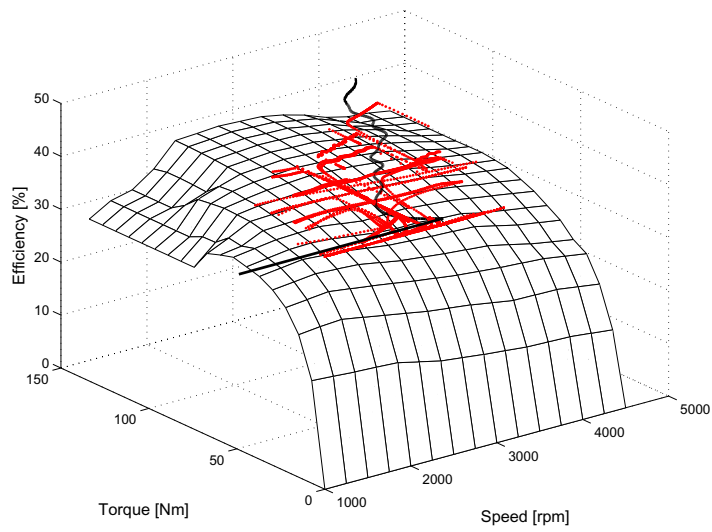
Figure 6.7:   The figure shows the *efficiency map* and results from simulation with the purpose to minimize NO_X emissions as control strategy. The optimal choice of load points considering best ICE efficiency is indicated as a solid black line. The chosen load points when driving ECE+EUDC are shown as red dots.
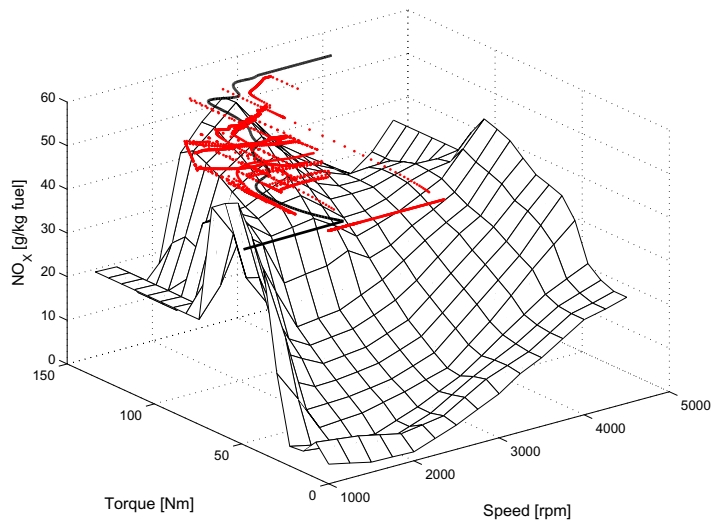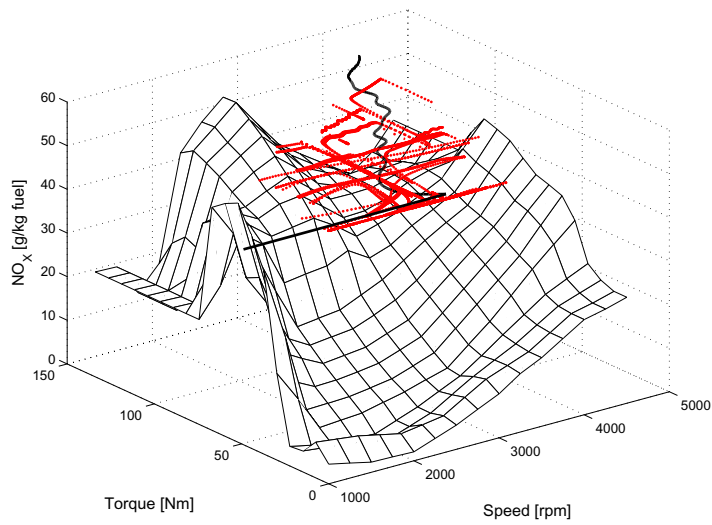
Figure 6.8:   The figure shows the *NO$_X$ emission map* and results from simulation with the purpose to minimize NO$_X$ emissions as control strategy. The optimal choice of load points considering lowest NO$_X$ is indicated as a solid black line. The chosen load points when driving ECE+EUDC are shown as red dots.
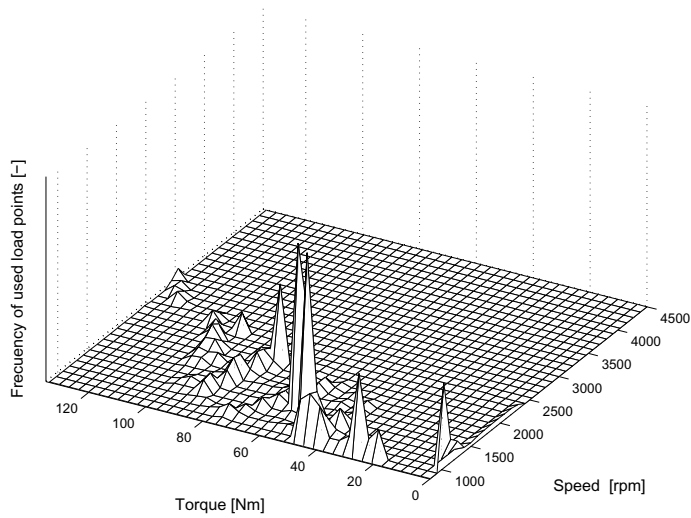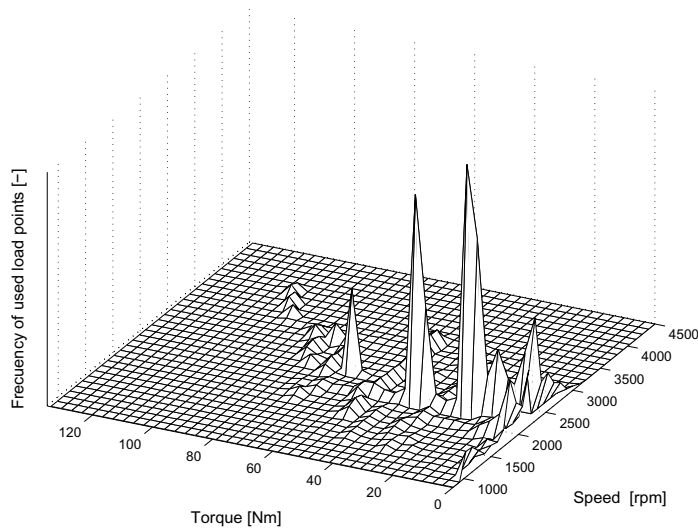
Figure 6.9:   The figure shows an operating diagram when simulating the driving
                ECE+EUDC with minimal NO_X as control strategy. The z-axis shows the
                frequency of how often the load points are used. Note that the main
                focus coincide with the optimum line (see Figure 6.7).

In Figure 6.10 it is however visible that the ICE efficiency optimized
control algorithm forces the engine to work at a higher efficiency – when
the ICE operates – compared to the NO_X optimized control algorithm.
When the ICE does not work, the battery supplies with the demanded
power. See Figure 6.11.
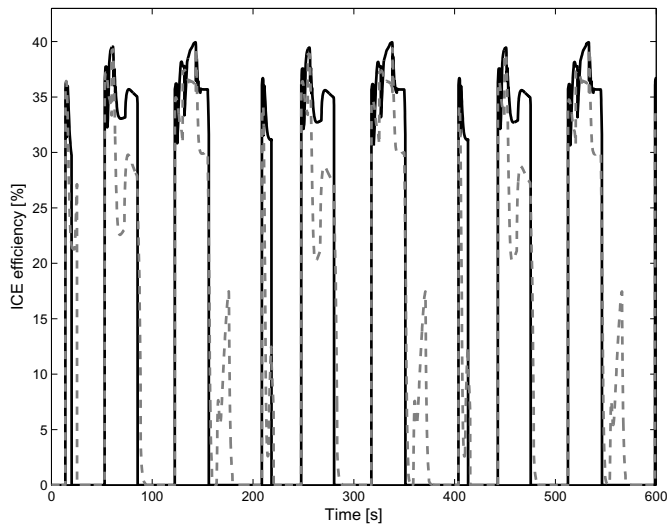
Figure 6.10: The figure shows ICE efficiency at 0 – 600 s, when running ICE efficiency optimized (black, solid) and NO_X optimized (grey, dashed).

The SOC indicates that the efficiency-optimized engine works at a higher ICE efficiency to the price of slightly larger deviations of SOC. See Figure 6.11. Simulations indicates nevertheless that this difference in SOC deviation, and the fuel consumption as well, would decrease if the losses in battery, power electronics and electric machines would decrease.
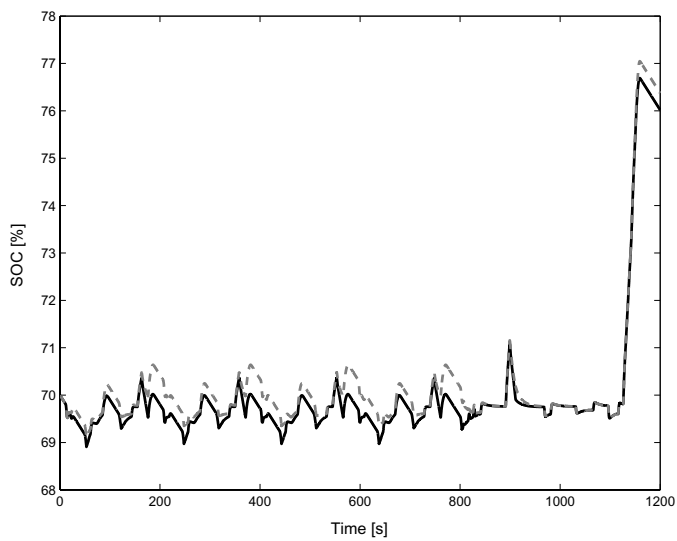
Figure 6.11:   The figure shows SOC when running ICE efficiency optimized (black,
solid) and NO$_X$ optimized (grey, dashed).

EGR

The results shown in Table 8 indicate that the original emissions control is poorly suited for the hybrid application. This can also be seen in Figure 4.4.

To handle this problem the EGR map is adjusted as shown in Figure 4.9. The amount of EGR is, all over the working area, equal to the highest amount EGR used anywhere in the conventional vehicle. The expected results hereof are reduced emissions at the expense of increased fuel consumption. The expectations are fulfilled, as can be seen in Table 9.

Table 9: Fuel consumption [l/100 km] and NO$_X$ [g/km] when running with increased EGR.

Optimization method:	Fuel consumption:	NO$_X$:
Efficiency:	4.4	1.33
NO$_X$:	4.9	0.69
Efficiency Max EGR:	5.1	0.33
NO$_X$ Max EGR:	5.7	0.25
Conventional:	5.6	1.03

SCR

With EGR, the emissions are still not reduced as much as needed to manage the Euro 4 regulations, when optimizing for ICE efficiency, and the intended limits of Euro 5, see Table 1, independently of chosen control strategy. Therefore SCR is implemented in the simulation model. The results can be seen in Table 10. The NO$_X$ conversion is temperature dependent as shown in Figure 4.15. The urea consumption is proportional to the amount of reduced NO$_X$.

Table 10: Fuel consumption [l/100 km] and NO$_X$ [g/km] when running with SCR. Urea consumption shown undiluted (normal dilution is 10% urea and 90% water) and in [g/km]. The price for the consumption of *Adblue*, the name under which urea is marked, is shown in [SeK/100km].

Optimization method:	Fuel consum.:	NO$_X$:	SCR Fuel consum.:	NO$_X$:	Urea consum. / Adblue:
Efficiency:	4.4	1.33	4.4	0.32	0.25 / 0.19
NO$_X$:	4.9	0.69	4.9	0.15	0.16 / 0.12
Efficiency Max EGR:	5.1	0.33	5.1	0.06	0.08 / 0.06
NO$_X$ max EGR:	5.7	0.25	5.7	0.07	0.05 / 0.04
Conventional:	5.6	1.03	-	-	-

The outcomes of these steps fulfil even the intended Euro 5 limits for NO$_X$ emissions (0.08 g/km). The fuel savings that the hybrid involves are slightly eaten up in the attempt to reduce the emissions. As mentioned in

Chapter 4.2 the emission reducing steps cost maybe less than these simulation indicates, at least not more.

Gear ratio and gearshift control

As can be seen in the previous results the control of the gearbox does not always permit the engine to work at optimum load points. One consequence is increased fuel consumption, especially when running the control algorithm for ICE efficiency optimization. If the ICE would be able to use the optimal load points, i.e. the vehicle would have been provided with a CVT, the results would be like those shown in Table 11 and Figure 6.12 - Figure 6.15. Note that the CVT in the simulation model is a rough model and does not include any losses of the CVT.

Table 11: Fuel consumption [l/100 km]] and NO_X [g/km] when running with CVT.

Optimization method:	Fuel consumption:	NO_X:
Efficiency:	4.4	1.33
NO_X:	4.9	0.69
Efficiency CVT:	4.3	1.35
NO_X CVT:	4.9	0.63
Efficiency Max EGR SCR CVT:	5.1	0.06
NO_X Max EGR SCR CVT:	5.8	0.07
Conventional:	5.6	1.03

Figure 6.12:   The figure shows chosen load points (red) and optimal load points (black) when controlling for optimal ICE efficiency.

Figure 6.13:   The figure shows an operating diagram when simulating the driving
                ECE+EUDC with optimal ICE efficiency as control strategy and using a
                CVT. The z-axis shows the frequency of how often the load points are
                used. Note that the main focus coincide with the optimum line (see
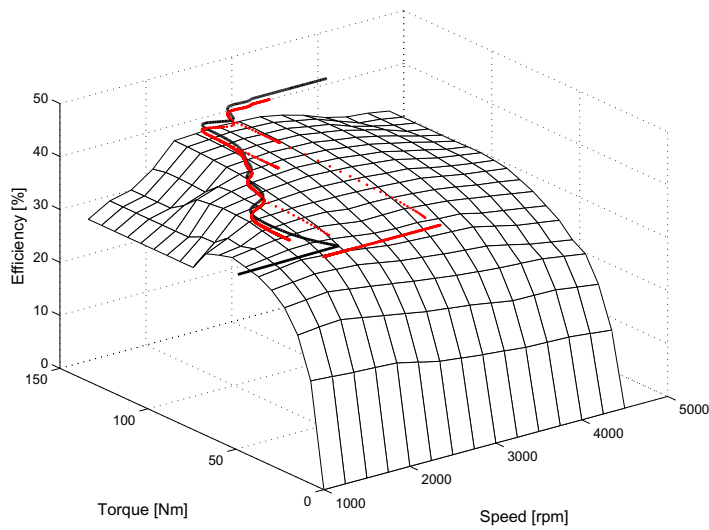   Figure 6.12).

Figure 6.14:   The figure shows chosen load points (red) and optimal load points
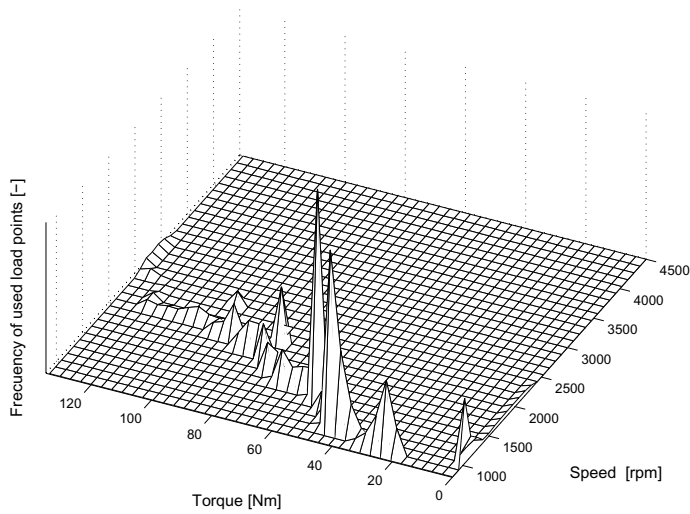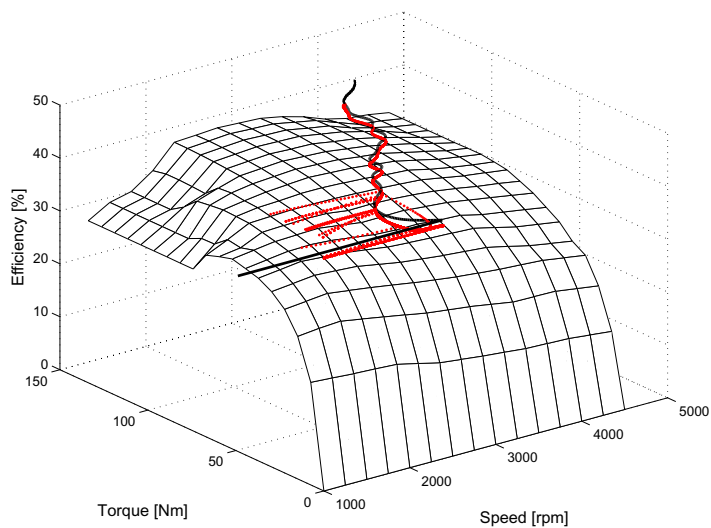   (black) when controlling for minimal NO$_X$.
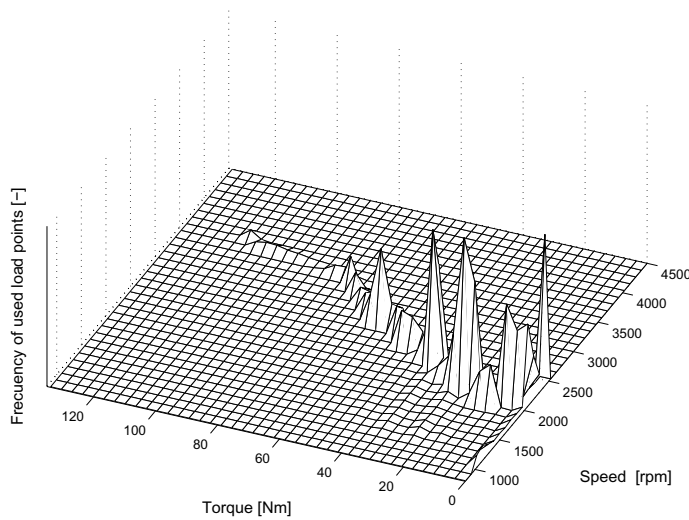
Figure 6.15: The figure shows an operating diagram when simulating the driving
ECE+EUDC with minimal NO_X as control strategy and using a CVT.
The z-axis shows the frequency of how often the load points are used.
Note that the main focus coincide with the optimum line (see figure
Figure 6.14).

As can be seen in Table 11 the fuel consumption does not change much
when optimizing for ICE efficiency, but the emission increases slightly
when running with CVT. This is due to the gained possibility to follow the
optimal load points and they imply increased NO_X emission.

When running for NO_X optimizing the emissions is reduced slightly more.
The question is why the NO_X does not decrease more, when it is allowed to
follow the optimal load points. The answer is that what is used, as the
optimal choice, is to some extent a middle course. The optimal choice of
load points does actually have the shape of a zigzag tread design.
Following that pattern would create undesired transients. Therefore the
outcome is evened up. The price for this can be seen in Table 11.

When running with maximum EGR, with SCR and with CVT it turns out
that the ICE efficiency optimization algorithm manages the NO_X reduction
even better than the control algorithm designed to reduce the NO_X
emission. This might be at a first glimpse surprisingly. The reason is found
in the SCR operation: The control strategy optimizing for minimum NO_X

operates at lower ICE efficiency. It also operates at lower temperature than the ICE efficiency-optimized strategy. Since the SCR is temperature dependent the NO_X reduction will hereby turn out slightly poorer.

The results indicate that it is of interest to adjust the gear ratio levels and the numbers of gears in the gearbox. Simulations are performed with adjusted final gear ratio, increased number of gears, adjusted shifting points and with adjusted gears. The adjustments affect both the fuel consumption as well as the emissions. This is due to changed load points involve changed output from the fuel- and emission maps.

Cylinder deactivation

Driving in city traffic demands less power than performing an overtaking at high speed. The latter can be a question of traffic safety. To be able to fulfil high power demand a sufficiently large engine has to be used. However when the power is not needed i.e. at low speed driving, the ICE efficiency quickly becomes very low. Including cylinder deactivation in the hybrid enables an increased ICE efficiency at low power demands. This is an implementation that can be done in conventional vehicles as well as in hybrid vehicles.

The results, when cylinder deactivation is included in the control algorithm for hybrid vehicles, are shown in Table 12.

Table 12: Fuel consumption [l/100 km] and NO_X [g/km] when running with deactivated cylinders.

Optimization method:	Max EGR and SCR		Cylinder deactivation, max EGR and SCR			
					CVT	
	Fuel consum.:	NO_X:	Fuel consum.:	NO_X:	Fuel consum.:	NO_X:
Efficiency:	5.1	0.06	4.9	0.05	4.9	0.05
NO_X:	5.7	0.07	5.9	0.05	6.0	0.05
Conventional:	5.6	1.03	-	-	-	-

Deactivating cylinders accentuate the earnings and weaknesses of the control strategies. The CVT allows the hybrid vehicle to operate close to the original choice of load points in the algorithms. The emissions are nevertheless slightly lower with the CVT, but sometimes only in the second or third digit. As seen in Table 12 the fuel consumption increase when the emissions decrease.

In Figure 6.16 the reason of increased fuel consumption when running with
NO_X controlled algorithm can be seen. The engine is operating in areas
with low NO_X at the price of reduced ICE efficiency, i.e. increased fuel
consumption.
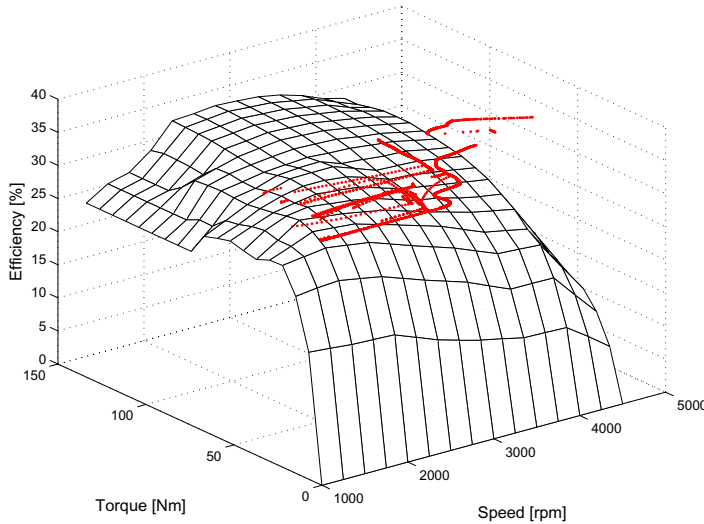
Figure 6.16:   The figure shows load points (red dots) when operating with maximal
EGR, NO_X optimized, with SCR and CVT and with the possibility to
deactivate. Note that some of the load points are for the deactivated
engine, i.e. the ICE efficiency will be increased compared to what is
actually visible in the figure. Nevertheless, the engine is working at low
ICE efficiency, which is visible when studying the fuel consumption in
Table 12.

The simulations with deactivated cylinders involve a decreased utilization
of the batteries since the ICE can be active even at low power levels
without loss of efficiency, thus reducing the need for electric traction. This
is due to that deactivated cylinders involve increased ICE efficiency at low
power demands. I.e. the engine is utilized more often, at high ICE
efficiency, and the losses in the battery, power electronics etc are decreased
due to reduced utilization. The SOC variations can be seen in Figure 6.17.
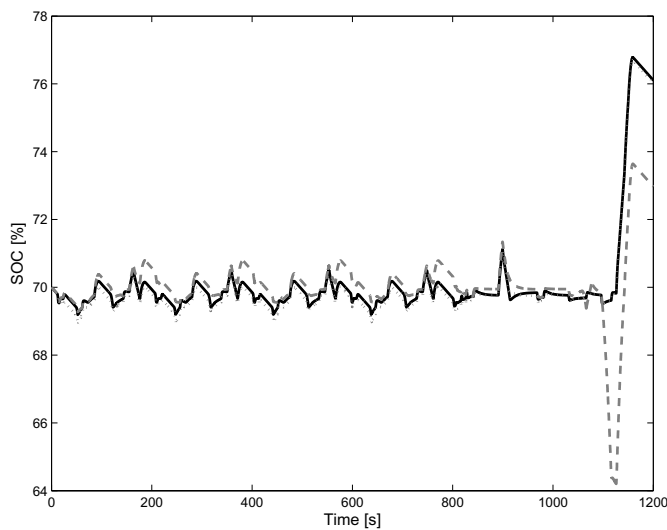
Figure 6.17:   The figure shows SOC when running with maximal EGR, ICE efficiency
optimized, with SCR and CVT with the possibility to deactivate (black,
solid), with maximal EGR, NO_X optimized, with SCR and CVT and with
the possibility to deactivate (grey, dashed), ICE efficiency optimized,
original EGR, no SCR, no CVT and no deactivation (grey, dotted).

As can be seen in Table 11 and Table 12 there are improvements to gain by utilizing cylinder deactivation. These simulations is carried out with two choices; all or half the number of cylinders. It is theoretically possible to deactivate one cylinder at a time, but it has not been implemented in this simulation model. Such a procedure would increase the possibilities to operate the ICE at a high average efficiency, i.e. reduce the fuel consumption even more. However, it is not realistic to deactivate any number of cylinders, since the mechanical balance is disturbed and undesired engine vibrations may occur.

These simulations have been performed on a city cycle, including a large amount of low speed driving. When driving a highway cycle the advantage of cylinder deactivation will not appear this distinctly due to increased power demand.

Addendum

Highway driving would however accentuate the difference between the control strategies. For example driving the highway cycle US06 implies

increased power demands due to higher speed and more aggressive accelerations, see Figure 6.18 and Figure 6.19. The US06 cycle is 12.8 km long, has a maximum speed of 130 km/h and a maximum acceleration of 3.24 m/s^2.
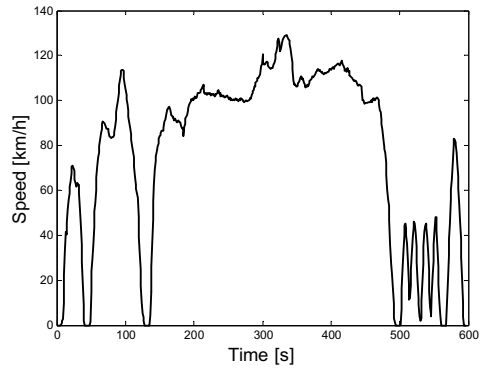
Figure 6.18:   Drive cycle US06, velocity.
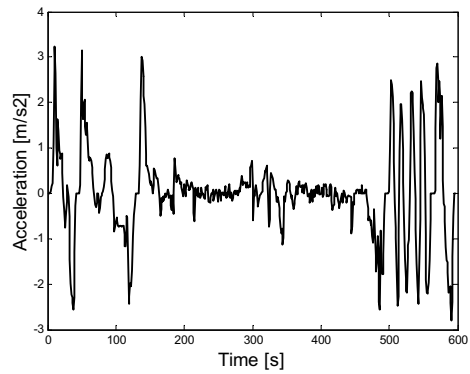
Figure 6.19:   Drive cycle US06, acceleration.

Since power is the product of torque and speed, large power demands high torque and high speed. The highway cycle implies a larger power demand, which in its turn leads to reduced freedom when choosing load points.

The raised power demands that this driving cycle implies, leads to that the differences in ICE efficiency and NO$_X$ optimization respectively is further investigated, see Table 13.

Table 13: Fuel consumption [l/100 km] and NO_X [g/km] when running the driving cycle US06 with deactivated cylinders.

| | Cylinder deactivation, max EGR and SCR | | | |
| | ECE+EUDC | | US06 | |
Optimization method:	Fuel consum.:	NO_X:	Fuel consum.:	NO_X:
Efficiency:	4.9	0.05	6.6	0.11
NO_X:	5.9	0.05	7.2	0.10

Running the highway cycle implies increased power demand and the fuel consumption increases herby.

The ICE efficiency optimized strategy implies especially increased emissions when the torque demand increases above all. It is still trying to follow the optimal choice shown in Figure 4.2. The consequences regarding NO_X can be seen in Figure 4.4.

Since the NO_X optimized strategy operates at load points including lower emissions at the expense of lower ICE efficiency, the fuel consumption increases further. The NO_X increases when the demanded power increases. The large power demand forces the engine to operate at load points with large emissions, see Figure 4.3. The emission savings that this control strategy involves is to some extent consumed, as can be seen in Table 13.

Chapter 7

Conclusions and future work

This thesis presents some of the opportunities diesel electric hybrid vehicles provide, but also some of the pitfalls that easily can destroy the benefits of hybridization. The simulation model used is a parallel hybrid as equal a Toyota Prius in engine and machine sizes, vehicle mass and shape etc as possible.

7.1 Summary of results

The main conclusion is that a conventional vehicle should not be converted into a hybrid vehicle without changes of its ICE control algorithms. Otherwise a great deal of the advantages of the hybrid application will get lost.

Control strategy

Hybrid vehicles involve a freedom of choice, but it is nevertheless necessary *to* choose load points of the ICE. Using an engine "of the shelf" implies using an ICE control strategy that does not take maximum advantage of hybridization. The ICE control strategy in a conventional vehicle rather counteracts the goal of hybridization. As shown in Table 8 the emission would not fulfil the regulations if not proper actions are taken.

The criterion for optimization should be selected with care. The results show two approaches: ICE efficiency and NO_X emissions. The outcome is not unambiguous. One should keep in mind that high ICE efficiency does

not necessarily imply low fuel consumption. It might mean that the battery is utilized to such an extent that the losses in the electric machine(s), battery, power electronics etc ruins the savings made by high ICE efficiency. A higher power demand has however a clear impact on the outcome, see Table 13. The determining factor when choosing the control algorithm must be for what purpose the algorithm is serving? A criterion often has to include compromises between various goals.

As can be seen in Table 8 the potential fuel savings when implementing hybridization amounts to 21%. This is apart from the fact that the emission might increase, as in the case with the ICE efficiency optimized control strategy. To obstruct this will affect the fuel consumption negatively on its hand.

EGR

The simulations show an adjustment of the EGR that is simple but also to some extent extreme. The aim is to investigate and point out the potential with adjusted EGR. The results show that extensive use of EGR has a significant potential concerning NO_X reduction.

The potential of NO_X reduction is, compared to a conventional vehicle equipped with a diesel engine, 68% (ICE efficiency controlled) and 76% (NO_X controlled) respectively. See Table 9. Unfortunately this improvement is not for free. The price to pay is 16% increased fuel consumption compared to not implementing adjusted EGR. The improvement compared to conventional vehicles is still 9% in fuel consumption when controlling for high ICE efficiency. When controlling for low NO_X the fuel consumption however increases 2% compared to conventional vehicle. There is a high price to pay to reduce the emission in this case. The method used for calculating the increase in fuel consumption when adjusting the EGR can be debated, but – the increase in estimated fuel consumption is pessimistic rather than optimistic. See Chapter 4.2.

SCR

Implementing SCR regarding reduced NO_X turns out as an effective measure for hybrid vehicles. The technology demands suitable temperature conditions, which is the case with hybrid vehicles.

As can be seen in Figure 4.15 the NO_X conversion is temperature dependent. The temperature in its turn depends on the chosen ICE load point. The optimization is carried out with intention to choose best temperature condition, regarding SCR. This can of course be tried out in further works. However the engine is working in the temperature region 250-450°C. The conversion has its peak at about 400°C. Hence follows that the SCR has the possibility to perform its intended use.

The reduction of NO_X when implementing only SCR is, for ICE and NO_X optimized respectively, 76 and 78%. Compared to using enlarged EGR the improvement is additional 81 and 72% respectively. Compared to a conventional vehicle the improvement is 94 and 93% respectively, in this case corresponding to 0.06 respectively 0.07 g NO_X/km, when implementing both EGR and SCR. One should keep in mind that the intended levels for NO_X emission in Euro 5 is proposed to be 0.08 g/km, which the NO_X optimized algorithm including SCR and enlarged EGR copes with.

Gearshift control

As shown in Table 11 the choice of gear ratios in the gearbox is important. One alternative could be a CVT, another more gears, yet an other increased lower gear ratios, since the ICE is supported by the electric drive an able to provide high wheel torque with increased gear ratio at the lower gear. The essential strategy is nevertheless to not use the solution the gearbox "off the shelf" provides with.

Last but not least, an adjusted gearshift control affects the emissions as well as the fuel consumption.

Cylinder deactivation

The gain of deactivating cylinders is primarily advantageous at low speeds, i.e. low power demands. This is due to the fact that the engine other wise is switched off and the electric path is utilized, which is causing losses. The possibility to increase the efficiency at low power demands – or reduce the NO_X further – improve the results even more when using cylinder deactivation. But in the case of optimizing for reduced NO_X the result is decreased ICE efficiency, i.e. the fuel consumption increases when the emission decreases.

When all possible adjustments are included (adjusted EGR, SCR, CVT and cylinder deactivation is added) the ICE efficiency optimized control algorithm saves 13% fuel and 95% NO_X compared to a conventional vehicle. When optimizing for NO_X the results turn out as a 7% increase of fuel consumption and 95% reduction of NO_X.

It turns out that the advantages gained by the NO_X minimizing algorithm when implementing NO_X emission treatment, with respect to NO_X reduction, is fully compensated for by the ICE efficiency optimizing control strategy. Since the NO_X minimizing algorithm operates at load points using lower ICE efficiency, the fuel consumption increases. The fuel consumption increases to such an extent that the emission savings will get lost.

The results presented above shows the potential the hybrid diesel electric vehicle possesses – when the possibilities it provides are utilized. It even makes it possible to fulfil the demands that Euro 5 is planned to signify, see Table 1 (Weissenberg, 2004 and European Union, 2005). However the hybrid vehicle is implemented with components that are not adapted to each other, the result will turn out poorer than the conventional alternative.

7.2 Future works

There are several subjects concerning control of hybrid electric vehicles that are not dealt with. Some interesting questions to investigate are suggested below.

The control strategy optimizing for ICE efficiency, does not consider the over all efficiency at all. An interesting study would therefore be to develop an algorithm that optimizes for the over all efficiency.

The hybrid vehicle in the simulation model is run on diesel fuel, but it would be interesting to study the efficiency and emission formation with bio fuels, like Ethanol or DME, when used in a hybrid vehicle.

Cylinder deactivation is used in this study to adapt the ICE power for low power requirements. Another solution could be using a small ICE that is strongly overcharged to handle the highest power requirements. The engine could in that case be provided with an electric turbo charger.

If the unit that distributes the demanded power to the electric machine(s) and the ICE would be able to predict the driving cycle, new possibilities open up. This would influence the usage of the batteries, i.e. there is a potential to reduce losses. One solution is to use a GPS that can predict the route. Another possibility is to use a control algorithm that by means of the last time period (μs/ms/s/min) can calculate a forecast of the demanded power.

This study presents a number of different parameters but only a limited number of possible alternatives and simulations. There are programs available which purpose is to find an optimized solution in a system containing a number of adjustable parameters. Such a procedure might be interesting to try out on this simulation model. All parameters investigated in the previous study (Jonasson, 2002) should also be included in such optimization.

When implementing cylinder deactivation, the necessity of a large battery decreases since the range of load points including high ICE efficiency increases. Therefore it would be interesting to carry out further investigations where the battery size is decreased.

A particular type of electric hybrid vehicles is called plug in-hybrids. The idea is to mainly utilize the electric machine(s) in these vehicles and mainly charge the battery from the grid. The ICE is more or less utilized as a range extender. An advantage with this, which would be interesting to investigate further, is the environmental potential it implies.

The optimization has not been carried out with intention to choose the best temperature condition, regarding SCR. This can of course be tried out in further works.

The received results points at the need of a control algorithm adjusted for hybrid implementation. It would therefore be valuable to perform measurements on the engine when the different control algorithms are implemented and adjusted. One questions to answer is, for example, what happens to the engine while large amount of EGR is used? How would the hybrid vehicle be affected by changes of the injection angle and other means of combustion control?

In the model it has been assumed that the included filter for PM is sufficient. It would be interesting to study this assumption closer, and to investigate the influence on the filter performance with higher EGR rates.

References

Al-Atabi, Mushtak Talib – Yusaf, Talal (2002), Experimental investigation of a single cylinder diesel engine as a hybrid power unit for a series hybrid electric vehicle, *Student conference on Research and development* (SCOReD 2002), Shah Alam, Malaysia.

Alaküla, Mats, Jonasson, Karin, Andersson, Christian, Simonsson, Bengt and Marksell, Sabine (2004), *Hybrid drive systems for vehicles, part 1*, Department of Industrial electrical engineering and automation, Lunds University, Lund, Sweden.

Andersson, Christian, Jonasson, Karin, Strandh, Petter and Alaküla, Mats (2000a), Simulation and verification of a hybrid bus, *NORPIE 2000*, Aalborg, Denmark.

Andersson, Christian (2001), *Observations on electric hybrid bus design*, Techn. Licentiate thesis, Department of Industrial electrical engineering and automation, Lund University, Lund, Sweden.

Andersson, Christian (2004a), *On auxiliary systems in commercial vahicles*, PhD thesis, Department of Industrial electrical engineering and automation, Lund University, Lund, Sweden.

Andersson, Jan, Axelsson, Roger and Jacobson, Bengt (2000b), Route adaptation of control strategies and driver assistant system for city buses, *International ImechE Conference "Bus 2000"*, London, Great Brittan.

Andersson, Lennart, Gabrielsson, Pär and Odenbrand, Ingemar (1994), Reducing NO_X in diesel exhaust by SCR technique: experiments and simulations, *A.I.Ch.E. Journal*, 1994, Vol. 40, No 11.

Andersson, Magnus (2004b), *An air hybrid capable of high power absorption and discharge*, Thesis of M Sc, Department of heat and Power Engineering, Lund University, Lund, Sweden.

Andreasson, Johan (2004), *Hybrid electric vehicles – aspects on driving dynamics and vehicle architecture*, Techn. Licentiate thesis, Department of Aeronautical and Vehicle Engineering, Royal Institute of Technology, Stockholm, Sweden.

Atkins, Matthew – Koch, Charles Robert (2003), A well-to-wheel comparison of several powertrain technologies, SAE 2003-01-0081, *SAE 2003 World Congress*, Detroit, USA.

Baretta, Joseph (1998), New classification on electric-thermal hybrid vehicles, *Electric Vehicle Symposium 15*, Brussels, Belgium.

Bengtsson, Johan (2004), *Closed-loop control of HCCI engine dynamics*, Department of Automatic Control, Lund University, Lund, Sweden.

Bolognesia, Paolo, Velerio Conte, Fiorentino, Lo Bianco, Giulia and Pasquali, Manlio (2001), Hy-Sim: a modular simulator for hybrid-electric vehicles, *Electric Vehicle Symposium 18*, Berlin, Germany.

Bosch (1996), *Automotive Handbook*, 4th edition, Germany.

Bäckström, Thomas (2000), *Integrated Energy Transducer Drive for Hybrid Electric Vehicles,* PhD-Thesis, Department of Electric Power Engineering, Electrical Machines and Power Electronics, Royal Institute of Technology, Stockholm, Sweden.

Challen, Bernard – Baranescu, Rodica (1999), *Diesel engine reference book*, 2nd edition, SAE, Warrendale, PA, USA.

Chan, Michael, Das, Sudhakar and Reitz, Rudolf (1997), *Modelling multiple injection and EGR effects on diesel engine emissions*, SAE 972864.

Chandler, Guy, Cooper, Barry, Harris, James, Thoss, James, Uusimäki, Ari, Walker, Andrew and Warren, James (2000), *An integrated SCR and continuously regenerating trap system to meet future NO_X and PM legislation*, SAE 2000-01-0188.

Chevron (2003-06-18), http://www.chevron.com/prodserv/fuels/bulletin/ diesel/L2_6_9_rf.htm.

Dieselnet (2001-03-14), http://www.dieselnet.com/standards/cycles/ ece_eudc.html.

Dieselnet (2004-12-16), http://www.dieselnet.com/standards/cycles/ ece_eudc.html.

Dieselnet (2005-01-12a), http://www.dieselnet.com/standards/cycles/ ece_eudc.html

Dieselnet (2005-02-25b), http://www.dieselnet.com/standards/eu/ld.html.

Duoba, Michael, Ng, Henry and Larsen, Robert (2001), Characterization and comparison of two hybrid electric vehicles (HEVs) – Honda Insight and Toyota Prius, SAE 2001-01-1335, *SAE 2001 World Congress*, Detroit, USA.

Eiraku, Akira, Abe, Tetsuya and Yamaoka, Masaaki (1998), An application of hardware in the loop simulation to hybrid electric vehicle, *Electric Vehicle Symposium 15*, Brussels, Belgium.

European Union (2005-02-28), http://www.europa.eu.int/comm/ enterprise/automotive/mveg_meetings/subgroup_euro/ meeting2/tax_incentives.pdf.

Gieshoff, A., Schäfer-Sindlinger, A., Spurk, P., van der Tillaart, J. and Garr, G. (2000), *Improved SCR systems for heavy duty applications*, SAE 2000-01-0189.

Green, Robert (2000), Measuring the cylinder-to-cylinder EGR distribution in the intake of a diesel engine during transient operation, SAE 2000-01-2861.

Gomez, Miguel, Mucino, Victor, Clarc, Nigel and Smith, James (2004), A configuration for a continuously variable power-split transmission in hybrid-electric vehicle applications, SAE 2004-01-0571, *SAE 2004 World Congress*, Detroit, USA.

Han, Zhang, Yuan, Zhu, Guangyu, Tian and Quanshi, Chen (2004), Optimal energy management strategy for hybrid electric vehicles, SAE 2004-01-0576, *SAE 2004 World Congress*, Detroit, USA.

Han, Zhiyu, Uludogan, Ali, Hampson, Gregory and Reitz, Rolf (1996) *Mechanism of soot and NO$_X$ emission reduction using multiple injection in a diesel engine*, SAE 960633.

Harbolla, B., Maggetto, Gaston, Van der Bossche, Peter and Van Muylem, H. (1992), Analyses of hybrid drive systems with new electric components – morphology, evaluation and optimisation, Institut für Kraftfahrwesen, RWTH Aachen, P-030 out of summary report Advanced electric drive systems for buses, vans and passenger cars to reduce pollution, EDS study, AVERE, Dec. 1992, Brussels, Belgium.

Heywood, John (1988), *Internal combustion engine fundamentals*, McGraw-Hill int. Editions, Automotive Techn. Series, Singapore.

Heilig, Mats (1985), *Kolvmaskiner AK*, (in Swedish), Department of Turbo machines, Lund University, Lund, Sweden.

Hellgren, Jonas (2004), *A methodology for the design of cost effective hybrid and fuel cell powertrains*, PhD thesis, Department of machine and vehicle system, Chalmers university of technology, Göteborg, Sweden.

Hellgren, Jonas – Jonasson, Karin (2004), Comparison of two algorithms for the energy management of hybrid powertrains, *NORPIE 2004*, Trondheim, Norway.

Hellman, Karl, Peralta, Maria and Piotrowski, Gregory (1998), Evaluation of a Toyota Prius hybrid system (THS), Technical Report EPA 420-R-98-006, United States Environmental Protection Agency, USA.

Hemmingsson, Morten (1999), *A powerflow control strategy to minimize energy losses in hybrid electric vehicles*, Techn. Licentiate thesis, Department of Industrial Electrical Engineering and Automation, Lund University, Lund, Sweden.

How stuff works, (2001-10-11a), http://www.howstuffworks.com/hybrid-car.htm.

How stuff works, (2001-10-11b), http://www.howstuffworks.com/question66.htm.

How stuff works (2005-02-17a), http://science.howstuffworks.com/fuel-cell.htm.

How stuff works (2005-02-17b), http://electronics.howstuffworks.com/motor.htm.

Imai, Sadoa, Takeda, Nobuaki and Horii, Yusuke (1997), Total efficiency of a hybrid electric vehicle, *Proceedings of the Power Conversion Conference*, Nagaoka, Japan, Aug. 3-6, vol. 2, pp. 947-950.

International Diesel Service (2005-03-15), www.ids.okq8.se.

INEEL (2002-02-02), http://ev.inel.gov/fop/general_info/aux2.html.

Johansson, Bengt (1999), *Förbränningsmotorer AK*, (in Swedish), Department of Heat and Power Engineering, Combustion Engines, Lund University, Lund, Sweden.

Johnson, Valerie, Wipke, Kieth and Rausen, David (2000), HEV Control Strategy for Real-Time Optimization of Fuel Economy and Emissions, SAE 2000-01-1543, *SAE 2000 World Congress*, Detroit, USA.

Johnson, Valerie, Zolot, Matthew and Pesaran, Ahmad (2001), Development and validation of a temperature-dependent resistance/capacitance battery model for ADVISOR, *Electric Vehicle Symposium 18*, Berlin, Germany.

Jonasson, Karin, Strandh, Petter and Alaküla, Mats (2001), Comparative study of generic hybrid topologies, *Electric Vehicle Symposium 18*, Berlin, Germany.

Jonasson, Karin (2002), *Analysing hybrid drive system topologies,* Techn. Licentiate thesis, Department of Industrial Electrical Engineering and Automation, Lund University, Lund, Sweden.

Jonasson, Karin, Alaküla, Mats and Egnell, Rolf (2003), Comparative study of petrol- and diesel hybrid topologies vs directly diesel driven vehicle, *Electric Vehicle Symposium 20*, Long Beach, USA.

Karlsson, Hua Lu (2000), Emission test of a Toyota Prius electric vehicle, Report No MTC6017, MTC AB, Haninge, Sweden.

Künkel, Christian (2001), *Catalytic Reduction of NO_X on heavy-Duty Trucks*, PhD-thesis, Department of Chemical Engineering II, Lund University, Lund, Sweden.

Liang, Chu, Weihua, Wang and Qingnian, Wang (2003), Energy management strategy and parametric design for hybrid electric military vehicle, SAE 2003-01-0086, *SAE 2003 World Congress*, Detroit, USA.

Lyshevski, Sergey Edward (1999), Diesel-electric drivetrains for hybrid-electric vehicles: new challenging problems in multivariable analysis and control, *IEEE International conference on control applications,* Hawaii, USA.

Maggetto, Gaston – Kahlen, Hans (1997), Electric and hybrid vehicles, *EPE -97*, Norway.

Van Mierlo, Joeri, Kamba Bimbi, Beya and Magetto, Gaston (1998), Comparison of power control algorithms in hybrid vehicles, *Electric Vehicle Symposium 15*, Brussels, Belgium.

Van Mierlo, Joeri (2000), *Simulation software for comparison and design of electric, hybrid and internal combustion vehicles with respect to energy, emissions and performances*, PhD-thesis, Department of Electrical Engineering, Vrije Universiteit Brussel, Brussels, Belgium.

Van Mierlo, Joeri – Magetto, Gaston (2000), Views on hybrid drivetrain power management strategies, *Electric Vehicle Symposium 17*, Montreal, Canada.

Miller, John M – Nicastri, Paul R (1998), The next generation automotive electrical power system architecture: issues and challenges, *The AIAA/IEEE/SAE Digital Avionics Systems Conference*, Seattle, USA.

Muta, Koichiro, Yamazaki, Makoto and Tokieda, Junji (2004) Development of new-generation hybrid system THS II – drastic improvement of power performance and fuel economy, SAE 2004-01-0064. *SAE 2004 World Congress*, Detroit, USA.

Nordlund, Erik (2003), *Simulation and design of a radial-radial four-quadrant transducer for hybrid electric vehicles*, Techn. Licentiate thesis, Department of Electrical Engineering, electrical Machines and Power Electronics, Royal Institute of Technology, Stockholm, Sweden.

Papadakis, Klaus (2003), *Exhaust gas cleaning by means of NOX storage and reduction technology on heavy-duty diesel vehicles*, Techn. Licentiate thesis, Department of Chemical Engineering, Lund University, Lund, Sweden.

Powertrain (2001-07-11), http://www.powertrain.se.

Rutquist, Per, Breitholtz, Claes and Wik, Torsten (2004), Optimal control of battery supercapacitor systems, *Reglermötet 2004*, Göteborg, Sweden.

Schechter, Michael. – Levin, Michael (1996), *Camless engines*, SAE 960581.

Stone, Richard (1999), *Introduction to internal combustion engines*, 3rd edition, SAE, Warrendale, PA. USA.

Strandh, Petter – Egnell, Rolf (2001), Modelling SI-engines for hybrid vehicles, SAE 2001-01-0575, *SAE 2001 World Congress*, Detroit, USA.

Strandh, Petter (2002), *Combustion Engine Models for Hybrid Vehicle System Development*, Techn. Licentiate thesis, Department of Heat and Power Engineering, Combustion Engines, Lund University, Lund, Sweden.

Stridsberg, Lennart (1998), Dual electric motor hybrid power train, *Electric Vehicle Symposium 15*, Brussels, Belgium.

Taylor, Charles Fayette (1982), *The internal combustion engine in theory and practice*, Cambridge, MA, USA.

Toyota Motor Corporation (2000), *PRIUS New Car Features*, May 2000, Pub. No. NCF 184E, Overseas service division, Toyota Motor Corporation, Japan.

Twike (2005-03-17), www.twike.ch.

U.S. Department of energy, Energy efficiency and renewable energy network (EREN) (2001-10-09), http://www.ott.doe.gov/hev/ what.html.

U.S. Environmental protection agency (EPA) (2005-02-25a), http://www.epa.gov/otaq/invntory/overview/pollutants/nox.htm#.

U.S. Environmental protection agency (EPA) (2005-02-25b), http://www.epa.gov/otaq/invntory/overview/pollutants/pm.htm

U.S. Environmental protection agency (EPA) (2005-02-25c), http://www.epa.gov/otaq/invntory/overview/pollutants/hydrocarbon s.htm.

U.S. Environmental protection agency (EPA) (2005-02-25d), http://www.epa.gov/otaq/invntory/overview/pollutants/carbonmon.h tm#.

Vedmar, Lars (1998), *Transmissioner*, (in Swedish), Department of Machine Elements, Lund University, Lund, Sweden.

Wang, Daxing – Zhang, Xin (2004), The development of powertrain control unit (PCU) for parallel hybrid electric vehicle (PHEV), SAE 2004-01-0575, *SAE 2004 World Congress*, Detroit, USA.

Weissenberg, Paul (2004), Euro 5 questionnaire, ENTR/F5 – PG/nb/ D(2003) 755842, European Comission, Entrprise Directorate-General, Brussels, Belgium.

Your dictionary (2001-10-09), http://www.yourdictionary.com/cgi-bin/mw.cgi.

Årzén, Karl-Erik (2000), *Real time control systems*, Department of Automatic Control, Lund University, Lund, Sweden.

Appendix A

Data according to Toyota Prius

The input data originate from Toyota (Toyota Motor Corporation, 2000) and are used as parameters in the simulation models. The main data are presented in Table 14.

Table 14: Data for Toyota Prius, used as parameters in the simulation models.

Property	Value
Vehicle mass (total) [kg]	1645
Front area [m^2]	2.52
Max power em1 [kW]	33
Max torque em1 [Nm]	350
Max speed em1 [rad/s]	585
Max power em2 [kW]	33
Max torque em2 [Nm]	68
Max speed em2 [rad/s]	471
Max power ICE [kW]	53
Max torque ICE [Nm]	115
Gear ratio ring wheel/wheel axis	3.5
Battery type	NiMH
Maximum charge [kWh]	1.7
Maximum speed [km/h]	160
Battery inner resistance [Ω][7]	0.49-0.56

---

[7] $R_{inner} = f(SOC)$ (Johnson et al., 2001)

Appendix B

Simulation model

The topmost level of the simulation model is shown in Figure 10.1. The implementation of the sub models, battery, ICE, electric machine etc, are described below.
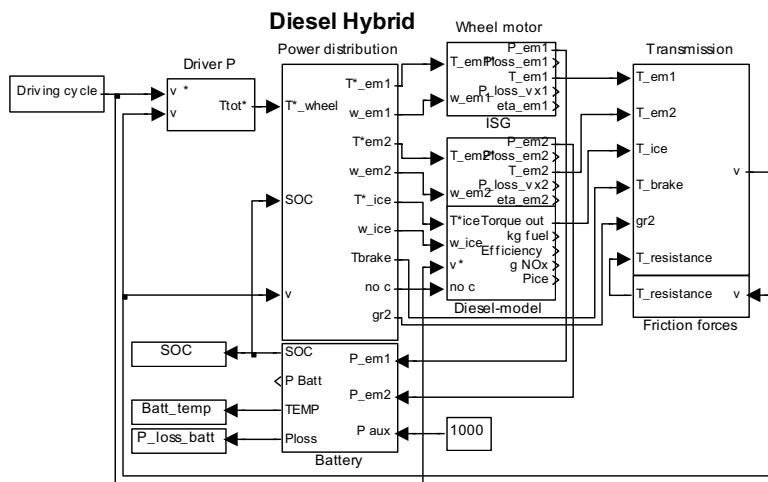

Figure 10.1:   The figure shows the topmost level in the simulation model. Each and every modelled subsystem forms a separate block.

Chassis dynamics

The chassis dynamics include both the transmissions and the friction forces, i.e. the air- and roll resistances etc.

The transmission model includes the basic equations for the gearboxes, including a fixed efficiency (99%) of each gear step. A 6 speed automatically shifted "manual" gearbox is used. The model inputs are torques and gear ratio. The model outputs are speed vehicle power. See Figure 10.2.
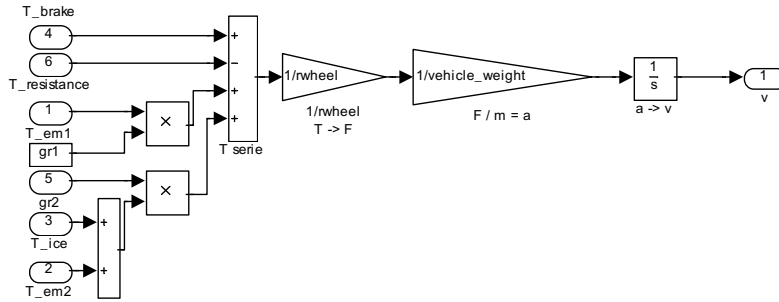

Figure 10.2:   The transmission block.

The road load is calculated by means of a formula originating from the vehicle industry. The formula is based on physical quantities deriving from the vehicle that includes the original diesel engine used in the simulation model. This vehicle is used as the reference vehicle when the model is validated. See Figure 10.3.
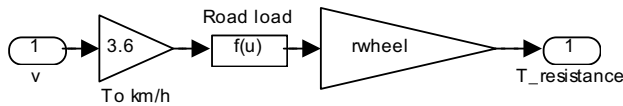

Figure 10.3:   The simulation block that considers the road load.

Input value in the block is the vehicle speed and output value is the resistance torque. The output signal, $T_{resistance}$, is thereafter inserted in the transmission block as a negative torque contribution.

Road slope, lateral and vertical forces have not been taken into consideration in the simulation model.

ICE

The ICE model included in the simulation model is built with the help of look-up-tables from a top of the art diesel engine as input data. The look-up-tables are scaled to fit the accurate engine size. The topmost level is shown in Figure 10.4.
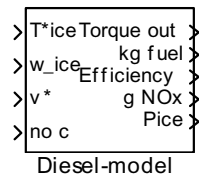

Figure 10.4:   The topmost level of the model of the diesel engine.

Inputs in the model are required torque, revolutions per minute, demanded speed and where appropriate, the number of cylinders (when using cylinder deactivation). Output values are torque and power. The model also calculates fuel consumption and emissions, which are the key parameters in this study.

Electric machines and power electronics

In these models the electrical machines and corresponding power electronics are represented together as a look up table of efficiency depending on speed (~ voltage) and torque (~current). In addition the maximum torque is limited taking field weakening operation into account. Transient torque boost is not represented.[8]

The electrical machines are modelled as a look up table with efficiency, where also the power electronic losses are included. This is motivated by the fact that speed and voltage are almost proportional in stationary

---

[8] Torque boost is the ability to transiently boost the torque from the electric machine at low speeds, above the actual maximum torque. This is only possible at limited time periods. The electric machine will otherwise obtain injurious temperatures due to the increased current.

operation. Moreover, current and torque are also almost proportional in stationary operation. Each electrical machine is given the efficiency characteristic shown in Figure 10.5, but the speed and torque axes that are scaled according to the specifications following chosen size of the electric machine.
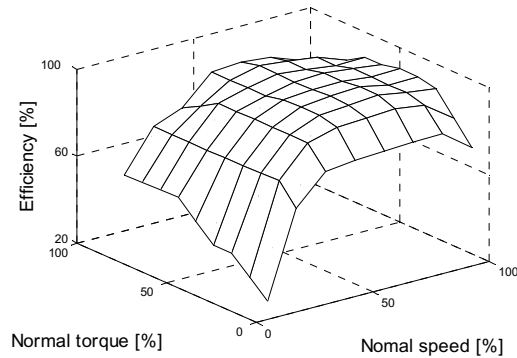

Figure 10.5:   The normalized value for efficiency, including the power electric losses, used in the electric machines.

The block inputs are the torque requirement, which originate from the power distribution block, and the present speed of the machine. The outputs consists of real supplied torque, power, gear- and machine losses. The block can be seen in Figure 10.6, where the look-up-table (shown in Figure 10.5) is visible in the centre of the simulation model.
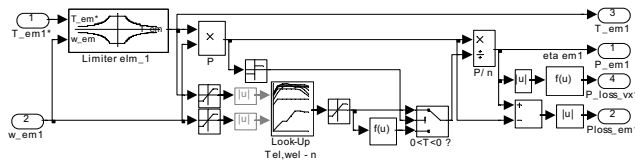

Figure 10.6:   The Simulink® block describing one of the electric machines.

Battery

The input values in the battery model are the power from the electric machines and the auxiliary that is a constant power representing light, air condition, fan etc. The size of P_{aux} is chosen with consideration to the

power consumption from the air condition published by Idaho National Engineering and Environmental Laboratory (INEEL, 2002). Depending on if the sum of power is positive or negative, the battery is charged or discharged.

Outputs from the sub model are battery temperature, battery losses, battery power and SOC, which has a reference value of 70% allow variations in SOC. See Figure 10.7. The SOC level is a result of the ICE control, i.e. the ICE is run at the best efficiency possible at any time and the battery is used as power compensator.
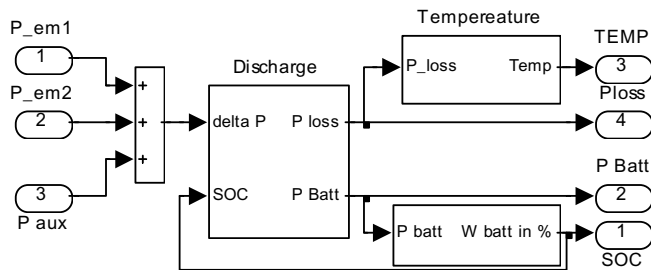

Figure 10.7:   The battery model.

The battery efficiency is dynamically adjusted depending on present values from SOC, battery current and voltage and the demanded ΔP. The battery inner resistance, R_{inner}, is depending on temperature and SOC. The temperature is assumed to be stable at +25°C. That means that R_{inner} is made only SOC dependent.

A thermal model is included in the sub model. It contains one thermal node inside the battery pack for a rough estimate of the battery temperature. This is then implemented in the following way in Simulink® (Figure 10.8):
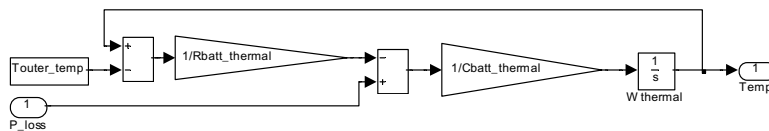

Figure 10.8:   The sub model to determine the battery temperature.

Driver model

In reality the driver reacts on a speed error and steps on the gas or the break depending on the sign of the speed error. The driver is modelled as a simple PI-controller, which reacts on the speed error, with anti-windup on the integrator to prevent saturation in the actuator.

There are three types of drivers to choose from in the simulation model; slow, normal and nervous. The differences between these driver types are the time before they react on a speed error (the time step) and the amplitude of the power demand. The "mode-factor" is a scaling factor of the size 0.5, 1.0 or 2.0.

The model is a rough and conscious simplification of the behaviour of a driver. The model is not checked against recorded driver behaviour, but this simplified driver is suitable for comparative studies, where the aim is the mutual results, not the definite figures.

The input values to the sub model are the driving cycle, i.e. the speed set point and the measured speed value. The output is the torque needed to minimize the speed error, i.e. if the driver needs to step on the gas or maybe break, see Figure 10.9 and Figure 10.10.
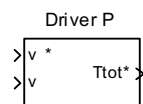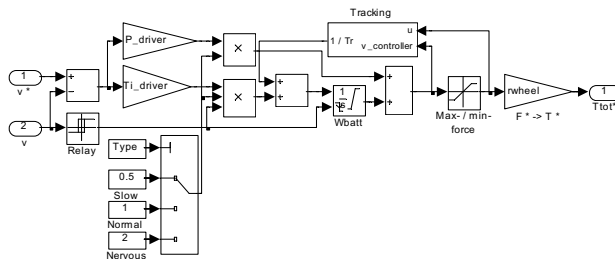

Figure 10.9:   Driver model.

Figure 10.10: Inside the driver block consisting the PI-controller.

Power distribution

This sub model represents the computing power used for control of the tractive energy flows onboard. All relevant quantities such as speeds, SOC etc. are used for calculation of the torque references for the ICE and the electrical machines, which are the model outputs.

The requested torques are depending on, i.e. the block inputs are, requested total torque, vehicle speed, speed of the ICE and SOC. This power distribution is valid for the parallel topology. If another topology would have been chosen, another power distribution should have been necessary.

Inside the block there is a hidden control system that calculates, optimises and distributes the requested torque for the electric machines and the ICE. This is dynamically calculated and the different boundaries are dynamically adjusted with respect to field weakening, efficiency etc. The complexity in the block makes showing the inside of the blocks more confusing than clarifying. Figure 10.11 shows consequently only the topmost level of the power distribution block in the model.
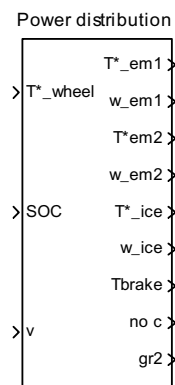
Figure 10.11: Power distribution block.

Driving cycle

This driving cycle block contains 13 driving cycles to choose from. Some of the cycles are internationally accepted standard cycles developed in different continents, and some are recorded locally in Sweden. Some are for buses and yet others are for private cars, see Figure 10.12. In this survey

not all cycles are used. The chosen cycle is the model input, as the simulated vehicle's attempt is to achieve the cycle speed. The single cycle consists of a look-up-table, where vehicle speed is a function of time.
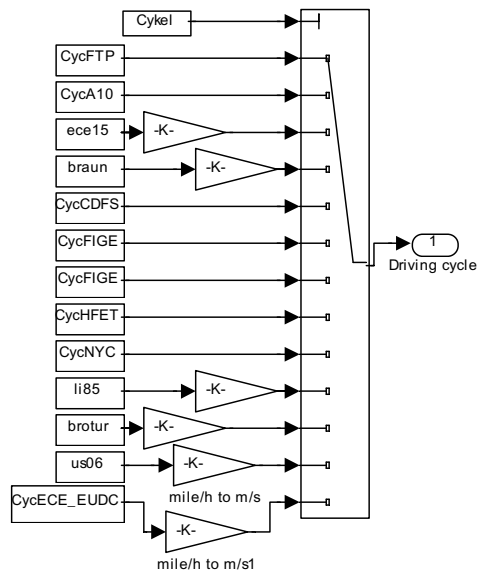
Figure 10.12: The driving cycle options.

Appendix C

Nomenclature and abbreviations

Abbrevations

A	air
BMEP	brake mean effective pressure
CO	carbon monoxide
CO₂	carbon dioxide
CVT	continuously variable transmission
DME	dymethyl ether
EGR	exhaust gas recirculation
EPA	Environmental protection agency
EREN	Energy efficiency and renewable energy network
EV	electric vehicle
F	fuel
FMEP	friction mean effective pressure
GDI	gasoline direct injection
GPS	Global positioning system
H	hydrogen
H₂O	water
HC	hydrocarbons
HEV	hybrid electric vehicle
ICE	internal combustion engine
IMEP	indicated mean effective pressure
NH₃	ammonia
NOₓ	nitrogen hydrogen oxides

n	net, all four strokes in a combustion cycle
O	oxygen
PM	particulate matter
PSH	power split hybrid
SCR	selective catalytic reduction
SOC	state of charge
TWC	three-way catalytic converter

Symbols

A_v	vehicle front area
$C_{batt\_thermal}$	thermal capacity
C_d	air resistance
C_r	rolling resistance
C_{r2}	second rolling resistance term
c_p	specific heat of a gas at constant pressure
c_v	specific heat of a gas at constant volume
e^-	electron
em_1	electric machine 1
em_2	electric machine 2
F_0, F_1, F_2	road load and aerodynamic losses
F^*_{tot}	total requested force
g	gravity
gr_1	gear ratio, gearbox 1
$gr_{1,min}$	gear ratio, gearbox 1, minimum value
$gr_{1,max}$	gear ratio, gearbox 1, maximum value
gr_2	gear ratio, gearbox 2
$gr_{2,min}$	gear ratio, gearbox 2, minimum value
$gr_{2,max}$	gear ratio, gearbox 2, maximum value
K_{Pice}	charging gain
P_r	resistance power
k	gain
M_v	vehicle mass
Nm	newton metre
P	power
P_{aux}	auxiliary power
P_{cool}	cooling power
P_{em1}	power, electric machine 1
P_{em2}	power, electric machine 2
P^*_{ice}	ICE power reference value
P_{loss}	power losses

P_{max}	maximum power
$P_{tractive}$	tractive power
P_r	resistance power
PE	power electronics
p	pressure
$R_{batt\_thermal}$	battery thermal resistance
r_{wheel}	wheel radius
rpm	round per minute
S_v	vehicle speed
SOC^*	state of charge reference
T	torque
T_{brake}	break torque
T_{em1}	torque, electric machine
T_{em2}	torque, electric machine 2
T^*_{em1}	torque reference value, electric machine
T^*_{em2}	torque reference value, electric machine 2
T_{emp}	battery temperature
T_{ICE}	ICE torque
T^*_{ICE}	ICE torque reference
T^*_{tot}	total requested torque
T_{outer}	outer temperature
$T_{resistance}$	resistance torque
u	actuator output
V	volume
V_D	piston displacement
v	velocity
v^*	velocity reference
$v_{controller}$	output of controller
$v_{vehicle}$	vehicle speed

Greek symbols

ε	compression ratio of an ICE
η_{em1}	efficiency of electric machine 1
η_{em2}	efficiency of electric machine 2
η_m	mechanical efficiency of an ICE
η_t	theoretical efficiency of a piston engine
κ	adiabatic exponent ($= c_p/c_v$)
λ	ratio between the amount of actual and stoichiometric fuel-to-air mixture
ρ_a	air density

τ_{ICE}	time constant
τ_i	integrator time constant
τ_t	tracking time constant
ω	speed
ω_{ice}	ICE speed
ω^*_{ice}	ICE speed reference value